Characterization of Alteration of Connexin-26 Through Lipid Bilayer to Evaluate its Role in Non-Syndromic Deafness

A Thesis submitted in the partial fulfillment of the requirements for the degree of

Master of Philosophy in Bioinformatics

By

Abida Batool

Supervisor

Dr. Sajid Rashid

National Centre for Bioinformatics

Faculty of Biological Sciences

Quaid-i-Azam University Islamabad, Pakistan

2016

CERTIFICATE

This thesis submitted by **Miss Abida Batool** from National Centre for Bioinformatics, Faculty of Biological Sciences, Quaid-i-Azam University, Islamabad, Pakistan, is accepted in its present form as satisfying the thesis requirement for the Degree of Master of Philosophy in Bioinformatics.

Internal Examiner:_____
Dr. Sajid Rashid
Associate Professor & Supervisor
Quaid-i-Azam University Islamabad.

External Examiner:_____
Dr. Muhammad Zeeshan Hyder
Assistant Professor
Department of Bio-Sciences,
COMSATS Institute of Information Technology
Islamabad.

Chairman:_____
Dr. Sajid Rashid
Associate Professor
National Centre for Bioinformatics
Quaid-i-Azam University Islamabad

Date:March 10,2016

DECLARATION

I hereby solemnly declare that the work **"Characterization of Alteration of Connexin-26 Through Lipid Bilayer to Evaluate its Role in Non-Syndromic Deafness"** presented in the following thesis is my own effort, except where otherwise acknowledged and that the thesis is my own composition. No part of the thesis has been previously presented for any other degree.

Dated: _____

Abida

Abida Batool

Dedicated to

My Beloved Family

Acknowledgement

Alhamdulillah, all praise to **Allah Almighty** who blessed me with knowledge and gave me the ability to use it during this research work. Praise and great gratitude to **Muhammad (S.A.W.W.)**, for his guidance towards the righteous path and for his teachings especially about seeking knowledge and spreading it.

First and foremost I offer my sincerest gratitude, special thanks and deep appreciation to my supervisor **Dr. Sajid Rashid** whose expertise, understanding, and patience, added considerably to my research experience. He was primary punch-bag and refinery for all my ideas and whose unceasing support throughout the conception, processing and completion of this study truly kept me going. I am grateful for his encouragement and practical advices. I am also thankful to him for reading my reports, commenting on my views and helping me understand and enrich my ideas. I appreciate his vast knowledge, vision and ethics which on many occasion made me "GREEN" with envy. I can't thank him enough for his tremendous support and help. He provided me with direction, technical support and became more of a mentor, than a supervisor. It was through his persistence, understanding and kindness that I completed my research work in time. I doubt that I will ever be able to convey my appreciation fully, but I owe him my eternal gratitude.

I am especially thankful to **Prof. Dr. Waseem Ahmad**, Dean of Biological Sciences and **Dr. Sajid Rashid**, Chairman of National Centre for Bioinformatics for letting me use this topic and providing me research facilities which made my research work possible. Their contribution in the form of stimulating suggestions and encouragement helped me coordinate my project.

I would like to thank my friends, particularly **Ayesha Hameed**, **Iqra Ahmad**, **Nimra Sabir**, **Noor UL Ain Sajid Mughal**, **Sehrish Ruba**, **Shabana Yasmeen Sundus Iqbal** and **Syeda Anber Zahra** for their kindness, moral support, joyful environment and venting of frustration during my study. Thanks for the friendship and ravishing memories.

I am also indebted to the members of the Functional informatics Lab, with whom I interacted during this research period. In my daily work, I have been so blessed to have such lively and cheerful colleagues. Particularly, I would like to acknowledge **Shabana Yasmeen**, **Shagufta Shafique**, **Muzammil Adeel**, **Muhammad Fakhar**, **Mehreen Jan**, **Hafsa Niyaz**, **Rafia Sajjad**, **Nazish Yasmeen**, **Shahida Batool**, **Khoula Rehman**, **Zainab Noor**, **Sana Tayyeb**, **Arwa Fiaz** and **Zunaira Asif**. Special thanks to **Saima Younas** who as a good friend, was always willing to help and give her best suggestions.

I am thankful to the system staff especially **Mr. Ali Raza** and **Mr. Yasir Ali Abbasi** for maintaining all the machines in lab so efficiently that I never had to worry about viruses, files loss, creating backups or installing softwares. I would like to acknowledge with much appreciation the crucial role of the whole staff of NCB including **Mr. Nasser Ahmad, Mr. Muhammad Naseer, Mr. Talib Hussain, Mr. Muhammad Yasir** and **Mr. Muhammad Kashif**.

Most importantly, none of this would have been possible without the love and patience of my family. My immediate family to whom this dissertation is dedicated to, has been a constant source of love, concern, support and strength all these years. I would like to express my heart-felt gratitude to my beloved parents; **Mr. Abdul Khaliq** and **Mrs. Zarina Khaliq** for their endless love, prayers, kindness, trust and support during my whole educational career. I would like to thank them for supporting me spiritually throughout my life.

Last but not least, my deepest gratitude goes to my brothers **Aamir Shafique**, **Ali Raza**, **Muhammad Adil Raza**, sisters **Asma Batool**, **Arfa Batool**, sister in law **Nazia Aamir**, my nieces **Samawal Batool**, **Anabiah Batool** and **Adn Batool** for their love, affection and encouragement during my study.

To those who indirectly contributed in this research, your kindness means a lot to me. Thank you very much.

Contents

List of Figures

List of Tables

List of Abbreviations

GJB2	Gap Junction Beta 2
Cxs	Connexins
Cx26	Connexin 26
HL	Hearing Loss
NSHL	Non-syndromic hearing Loss
IP3	Inisitol triphosphate
$Cx26^{WT}$	Connexin-26 Wild Type
$Cx26^{MUT}$	Connexin-26 Mutated
DPPC	Dipalmitoylphosphatidylcholine
MD	Molecular dynamics
HCs	Hemichannels
GJCs	Gap junction channels
TM	Transmembrane helices
RMSD	root mean square deviation
RMSF	root mean square fluctuation
Rg	radius of gyration

Aminoacid	**Three letter code**	**Single letter code**
Alanine	Ala	A
Arginine	Arg	R
Asparagine	Asn	N
Aspartate	Asp	D
Cystine	Cys	C
Lysine	Lys	K
Glutamate	Glu	E
Glycine	Gly	G
Gutamine	Gln	Q
Histidine	His	H
Isoleusine	Ile	I

Leucine	Leu	L
Metionin	Met	M
Phenylalanine	Phe	F
Proline	Pro	P
Serine	Ser	S
Valine	Val	V
Tyrosine	Tyr	Y
Therionine	Thr	T
Tryptophan	Trp	W

Abstract

Connexin26 (Cx26) is a β-class gap junction protein expressed in the cochlea, inner ear and in the epidermis. Mutations in Cx26 are responsible for at least 20% of all genetic hearing loss and 10% of all childhood hearing loss. Gap junctional proteins join together at their extracellular membrane and form intercellular channels, permitting the distribution of K+ and Ca^{2+} ions, second messengers (e.g., cAMP and inositol 1,4,5-triphosphate), and small metabolites (e.g., glucose) that are essential for normal cellular development and functions. Any damage to these gap junctions would lead to the disturbance of equilibrium of the cells which may result in various diseases. The majority of mutations that cause non-syndromic hearing loss are responsible for either generalized folding problems resulting in the failure of Cx26 movement to the cell surface, or are permissive for the formation of gap junction, which prevent intercellular channel functions. It is important to analyze the entire environment for a large class of biomolecular processes, i.e., those that take place within biological membranes. Current study establishes the use of structural proteomics and molecular dynamics simulation studies to identify the alterations in Cx26 structure and its interactions with membrane lipid due to T8M mutation that is the major cause (6.1%) of inherited deafness in the Pakistani population. 3-dimensional structure of $Cx26^{MUT}$ protein was generated through homology modeling via MODELLER. Then it was used to explore the differences in transmembrane topology and gap junctional tunnel between wild type and mutated Cx26. MD simulation results revealed that the $Cx26^{WT}$ was more stable as compared to the $Cx26^{MUT}$ protein. T8M mutation resulted structure instability and reduced functionality due to which second messenger are no more able to pass through Cx26 creating functional disturbances leading to non-syndromic deafness.

INTRODUCTION

1. Introduction

Deafness or hearing loss (HL) is a sensory disability to perceive sounds. Hearing impairment effects millions of people all over the world. Although it is not life threating but it can be a major problem in social and professional life (Kemperman *et al.*, 2002). Deafness is affecting almost 600 million people in the world (Traynor *et al.*, 2011), and it is the most common genetic abnormality, affecting 2 to 6 per 1,000 neonates (Traynor *et al.*, 2011, Morton *et al.*, 1991). At least two-thirds of these cases in the world are inherited while the remaining one-third is attributed to environmental and infective factors (Hilgert *et al.*, 2009).

1.1 Types of deafness

Deafness can be distinguished as Syndromic and Non-Syndromic deafness depending on whether other distinctive physical features are present or absent respectively. Non-Syndromic deafness doesn't include any other abnormality and is typically sensorineural (Bitner-Glindzicz *et al.*, 2002), while syndromic deafness can be sensorineural, conductive, or mixed. This type of deafness includes additional disability like cognitive impairment (Van-Naarden *et al.*, 1999) or cardiac dysfunction (Baig *et al.*, 2011). Almost 400 syndromes include hearing loss as a part of their phenotypic signature (Hilgert *et al.*, 2009).

Most inherited forms of deafness segregate as monogenic traits but digenic inheritance has also been reported (Zheng *et al.*, 2005). Based on the mode of inheritance, monogenic hearing loss is categorized as autosomal recessive, autosomal dominant, X-linked, and mitochondrial (Cryns *et al.*, 2004). Epidemological features determine that prelingual deafness is 0.2-0.6%, genetically caused 50%, syndromic 25%, non-Syndromic 75%, autosomal dominant 20%, autosomal recessive 74%, X-linked 5% and mitochondrial is 1% (Kemperman *et al.*, 2002).

1.2 Genes associated with deafness

Deafness is genetically heterogeneous disorders, with more than 100 mapped loci and more than 60 genes are located in these loci (Van-Camp *et al.*, 2012). It is expected that approximately 1% of human genes play a role in hearing (Friedman *et al.*, 2003). By genetic linkage technique, many non-syndromic forms of deafness have been localized on the

human genome since 1997. These loci include DFNA (autosomal dominant), DFNB (autosomal recessive) and DFN (X-linked), depending upon the pattern of inheritance (Kemperman *et al.*, 2002).

Deafness is more common in developing countries of Asia. Like other genetic disorders, deafness has high occurrence among consanguineous populations (Zakzouk *et al.*, 2002). Pakistan, where >60% marriages take place within families, has high frequency of deafness (Hussain and Bittles *et al.*, 1998). Pakistani population is one of the richest genetic resources to study inherited deafness. More than 35 autosomal recessive non-syndromic loci have been mapped in Pakistan (Riaz and Iqbal *et al.*, 2012). Deafness is higher in the Pakistani population (0.16%) than rest of the world (average 0.1%) due to high consanguinity (Hussain and Bittles *et al.*, 1998).

Genes that are more frequently involved in inherited deafeness in Pakistan are mentioned in table 1.1.

Table 1.1: Genes involved in causing deafness in Pakistan.

Gene name	Locus	Reference	Incidence of Deafness
MARVELD2	DFNB49	Nayak *et al.*, 2015	1.5%
LRTOMT	DFNB63	Ahmed *et al.*, 2008	0.5%
CDH23	DFNB12	Bork *et al.*, 2001 Riaz *et al.*, 2012	5%
TMC1	DFNB7 DFNB11	Kitajiri *et al.*, 2007 Santos *et al.*, 2005	3.4% 4.4%
C9orf75(TPRN)	DFNB79	Rehman *et al.*, 2010	0.25%
TRIOBP	DFNB28	Riazuddin *et al.*, 2006	1.6%
RDX	DFNB24	Khan *et al.*, 2007 Ali *et al.*, 2010	0.3%
MYO6	DFNB37	Ahmed *et al.*, 2003	1.2%
MYO15A	DFNB3	Nal *et al.*, 2007 Riaz *et al.*, 2012	5%

MSRB3	DFNB74	Ahmed *et al.*, 2011 Waryah *et al.*, 2009	1.1%
PJVK	*DFNB59*	Mujtaba *et al.*, 2012	0.8%
GJB2	DFNB1 DFNA3	Anjum *et al.*, 2014 Padma *et al.*, 2009 Brown *et al.*, 1996	6.1%
SLC26A4	DFNB4	Anwar *et al.*, 2009 Park *et al.*, 2003	5.2%
TMPRSS3	DFNB8 DFNB10	Ahmed *et al.*, 2004	1.8%
TMIE	DFNB6	Naz *et al.*, 2002	1.3%
CIB2	DFNB48	Riazuddin et al., 2012 Ahmad *et al.*, 2005	1.5%
MYO7A	DFNB2	Riazuddin *et al.*, 2008	3.5%
ESRRB	DFNB35	Collin *et al.*, 2008	0.6%
ILDR1	DFNB42	Borck *et al.*, 2011	0.5%
HGF	*DFNB39*	Schultz *et al.*, 2009	2.1%
OTOF	*DFNB9*	Choi *et al.*, 2009	2.3%

Gap Junction Beta 2 (*GJB2*) mutations are the major cause of inherited deafness and are accountable for >50% of non-syndromic deafness (Chen *et al.*, 2014). Although it is involved in autosomal dominant form of deafness (DFNA3), most of its mutations result in autosomal recessive deafness (DFNB1) (Cohn *et al.*, 1999, Denoyelle *et al.*, 1999). DFNB1 is the 1st locus which is involved in autosomal recessive non-syndromic deafness and gene present on this locus is *GJB2* (Kelsell *et al.*, 1997). *GJB2* is a small gene located at the chromosomal location: (GenBank M86849, OMIM: *121011) 13q11. It is 5.5 kbp long and has two exons but only one of them has coding sequence. The mRNA is 2.4 kbp long and encodes Connexin26 (*Cx26*) protein (Kelley *et al.*, 2000).

1.3 Connexin protein family

Connexins belong to a large family of transmembrane proteins which allow intercellualar communication (Dbouk *et al.,* 2009). Human Connexin family comprises of 21 members, each encoded by a different gene. These are divided into five distinct subgroups, named as α, β, γ, δ and ε (Bosco *et al.,* 2011). Phylogenetic tree of Connexin family is given in figure 1.1.

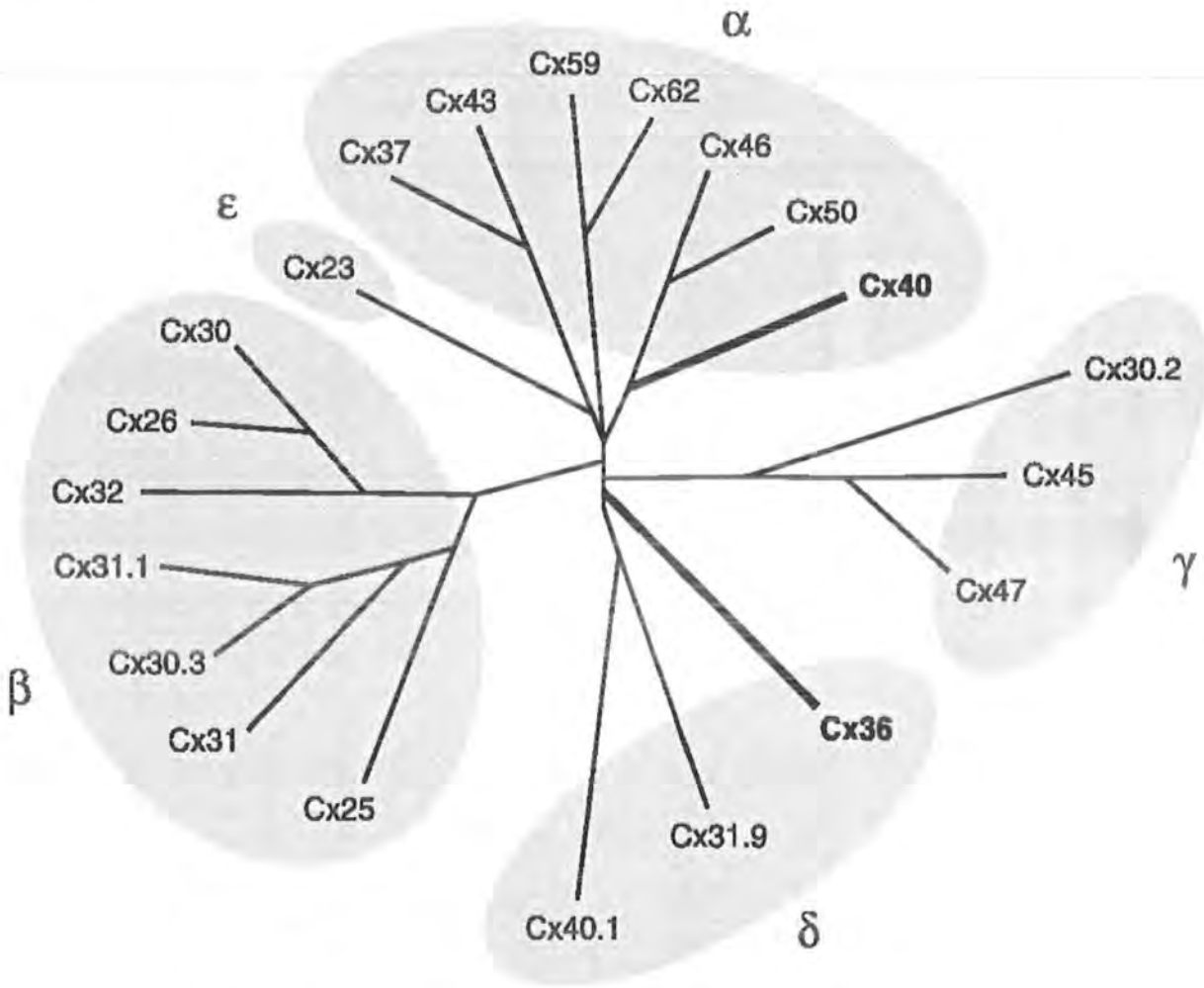

Figure 1.1: Phylogenetic tree of Connexin family (Bosco *et al.,* 2011).

Connexins (Cxs) are expressed in almost every cell type in the human body (Bruzzone *et al.,* 1996) such as *Cx43*, which is found in the brain, kidneys, heart and reproductive organs, among others (Saez *et al.,* 2003), *Cx29* is restricted to myelin-forming glial cells, (Sohl et al., 2001) or *Cx26* and *Cx30* in the inner ear. Cxs form two types of channels; hemichannels

(HCs) and gap junction channels (GJCs). HCs are formed by the oligomerization of six Cxs monomers and travel through vesicles to the plasma membrane (Vinken et al., 2006, Laird *et al.,* 2006). Connexins HCs and GJCs arrangement in plasma membrane is shown in figure 1.2.

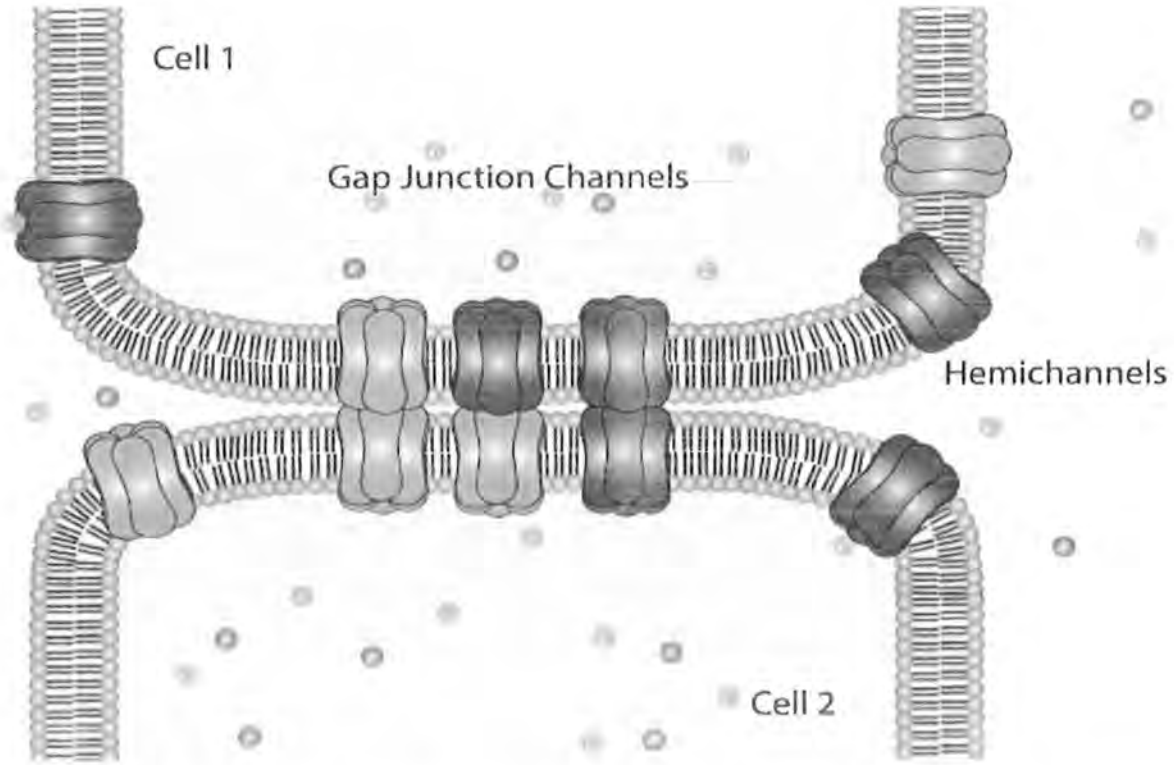

Figure 1.2: Plasma membrane arrangements of Cxs (Retamal *et al.,* 2015). Six Cxs oligomerize to form a HC that traveled to the plasma membrane to form free HCs, which provide a communication pathway between the cell and the extracellular environment. Alternatively, can dock others HCs provided by an adjacent cell (appositional plasma membrane) to form intercellular aqueous pore named GJCs.

Connexin25 (*Cx25*), Connexin26 (*Cx26*), Connexin30 (*Cx30*), Connexin31 (*Cx31*), Connexin36 (*Cx36*), Connexin40 (*Cx40*), Connexin43 (*Cx43*), Connexin46 (*Cx46*) are all involved in non-syndromic deafness. *Cx26* is responsible for at least 20% of all genetic hearing loss and 10% of all childhood hearing loss. *Cx26* is a β-class gap junction protein expressed in the cochlea and in the epidermis (Kelsell *et al.,* 1997). It has 226 aminoacids (Kelley *et al.,* 2000). It consists of six chains that form a hexamer complex called connexon.

Two hexamers in membrane of adjacent cells form a cell to cell channel or a tunnel called as gap junction (Kikuchi et al., 2000). Each chain consists of four transmembrane helices (TM1-TM4), two cytoplasmic loop and one extracelluar loop. Each connexin has a positively charged cytoplasmic entrance, a negatively charged transmembrane pathway and an extracellular cavity (Maeda *et al.*, 2009).

1.4 Cx26 mutations associated with deafness

Mutations in Cx26 and their frequencies are largely dependent on ethnicity (Yilmaz et al., 2010). Mutations in Cx26 that cause non-syndromic deafness are mentioned in table 1.2.

Table 1.2: Cx26 mutations that are responsible for deafness.

Codon location	Mutation type	Reference
M1V	Missense	Estivill *et al.*, 1998
T8M	Missense	Anjum *et al.*, 2014
35delG	Deletion /frameshift	Carrasquillo *et al.*, 1997 Denoyelle *et al.*, 1997 Zelante *et al.*, 1997
31–68del(38)	Deletion/frameshift	Denoyelle *et al.*, 1997
35insG	Insertion/frameshift	Estivill *et al.*, 1998
W24X	Non-sense	Kelsell *et al.*, 1997
V27I	Variant	Kelley *et al.*, 1998
M34T	Missense	Kelsell *et al.*, 1997
V37I	Variant	Kelley *et al.*, 1998
W44C	Missense	Denoyelle *et al.*, 1998
E47X	Non-sense	Estivill *et al.*, 1998 Denoyelle *et al.*, 1997
167delT	Deletion /frameshift	White *et al.*, 1998
V52L	Missense	Snoeckx *et al.*, 2005
Q57X	Non-sense	Snoeckx *et al.*, 2005
V63M	Missense	Snoeckx *et al.*, 2005
Y65X	Non-sense	Estivill *et al.*, 1998

R75W	Missense	Rabionet *et al.*, 1998
W77R	Missense	Carrasquillo *et al.*, 1997
W77X	Non-sense	Padma *et al.*, 2009
Q80P	Missense	Snoeckx *et al.*, 2005
I82M	Missense	Snoeckx *et al.*, 2005
235delC	Deletion /frameshift	Scott *et al.*, 1998
V84L	Missense	Kelley *et al.*, 1998
267insT	Insertion/frameshift	Green *et al.*, 1999
L90P	Missense	Snoeckx *et al.*, 2005
V95M	Missense	Kelley *et al.*, 1998
R98Q	Missense	Green *et al.*, 1999
H100Y	Missense	Green *et al.*, 1999
314–327del 14	Deletion /frameshift	Kelley *et al.*, 1998
333–334del(AA)	Deletion /frameshift	Kelley *et al.*, 1998
S113R	Missense	Scott *et al.*, 1998
358del(GAG)	Deletion /frameshift	Denoyelle *et al.*, 1997
R127H	Missense	Estivill *et al.*, 1998
L132V	Missense	Snoeckx *et al.*, 2005
S139N	Missense	Snoeckx *et al.*, 2005
R143W	Missense	Scott *et al.*, 1998
E147K	Missense	Snoeckx *et al.*, 2005
510insA	Insertion/frameshift	Denoyelle *et al.*, 1997
F161S	Missense	Rabionet *et al.*, 1998
P173R	Missense	Rabionet *et al.*, 1998
R184P	Missense	Rabionet *et al.*, 1998
572delT	Deletion /frameshift	Murgia *et al.*, 1999
S199F	Missense	Green *et al.*, 1999
631–632del(GT)	Deletion /frameshift	Kelley *et al.*, 1998
N206S	Missense	Snoeckx *et al.*, 2005
T208P	Missense	Snoeckx *et al.*, 2005

1.5 Connexin passage through lipid bilayer

Lipids provide a structural and functional framework to all membrane proteins (Locke *et al.*, 2009). Interactions of membrane proteins with membrane lipids are of structural and functional significance (Lee *et al.*, 2004). Proteins of Connexin family are known for their ability to form hexamers in the plasma membrane. These hexameric proteins join together at their extracellular membrane and form intercellular channels (Harris *et al.*, 2008). Intercellular channels cluster together to form gap junctions that are typically long, distinct at the specified regions of plasma membrane. The lipid composition of this portion differs from surrounding plasma membrane. HCs and GJCs are shown in Figure 1.2. Gap junctions directly bind with the cytoplasam of adjacent cells, permitting the distribution of K^+ and Ca^{2+} ions, second messengers (e.g., cAMP and inositol 1,4,5-triphosphate (IP3)), and small metabolites (e.g., glucose) that are essential for normal cellular development and functions (Lawrence *et al.*, 1978 , Malewicz *et al.*, 1990). The majority of mutations that cause non-syndromic hearing loss are responsible for either generalized folding problems that result in the failure of Cx26 movement to the cell surface, or are permissive for the formation of gap junction, but prevent intercellular channel functions (Xu *et al.*, 2013).

1.6 Comparative modelling

Functional characterization of a protein sequence is one of the most frequent problems in biology. This problem can be solved by accurate three-dimensional structure of the protein. In the absence of an experimentally determined structure, comparative modelling or homology modelling is a useful method to model three-dimensional protein structures using experimentally determined structures of related family members as templates (Eswar *et al.*, 2006). Building homology models involves specialized programs and up-to-date sequence and structural databases (Arnold *et al.*, 2005). Many web-based as well as offline desktop tools can be used for homology modelling. SWISS-MODEL (*http://swissmodel.expasy.org*), Geno3D (*http://geno3d-pbil.ibcp.fr*), ESyPred3D (*http://www.fundp.ac.be/urbm/bioinfo/esypred/*), 3D-JIGSAW (*http://bmm.crick.ac.uk/~3djigsaw/*), CPHModel (*http://www.cbs.dtu.dk/services/CPHmodels/*) and PHYRE2 (*http://www.sbg.bio.ic.ac.uk/phyre2/html/page.cgi?id=index*) are some of the common

web based homology modelling servers. FoldX, Prime, CABS, RaptorX and MODELLER are some easy downloadable desktop tools for comparative modelling.

1.7 Lipid bilayer simulation

Over the last few decades, molecular dynamics simulation has become a common tool in theoretical studies of simple liquids as well as large biomolecular systems such as proteins or DNA in real world solvent environments. By this technique, statistical properties such as free energy of solvation or binding of small molecules and protein folding rates etc. can be extrapolated (Hess *et al.*, 2008). It is important to analyse the entire environment for a large class of biomolecular processes, i.e., those that take place within biological membranes (Israelachvili *et al.*, 1980). Despite complete information of 3D structures of membrane proteins, many of the factors responsible for the conformational stability of membrane proteins are still not well understood. The complications in finding detailed information at the molecular level about the phospholipid bilayer environment and its influence on lipid-protein interactions contribute to the problem. The main effect on the membrane is that of a thermodynamic driving force involved in partitioning the amino acids according to their solubility i.e. hydrophobic amino acids are more likely to be found within the core of the membrane whereas charged and polar amino acids are more likely to be found in the bulk solvent (Terwilliger *et al.*, 1982, Wesson *et al.*, 1992). Molecular dynamics (MD) simulation assay of complete atomic models based on the realistic microscopic interactions is a powerful tool to gain insight into the structure and dynamics of complex macromolecular systems such as membrane proteins (Brooks *et al.*, 1990). Simulations of lipid bilayers, biomembranes and related systems by MD (Haile *et al.*, 1992) and Monte Carlo (Mooney *et al.*, 1997) is an area of rapid growth (Pastor *et al.*, 1994). The membrane environment effects the function of membrane proteins through electrostatic and steric interactions as well as through the membrane's internal pressure. Therefore, the environment needs to be properly taken into account in MD studies (Gumbart *et al.*, 2005). One drawback of the membrane simulation approach is that its success depends on various methodological issues such as force fields, constraints, and the accuracy of incorporation orders for the equations of motion (Tieleman *et al.*, 1997; Chiu *et al.*, 2000; Besold *et al.*, 2000; Vattulainen *et al.*, 2002). In particular, the treatment of electrostatic interactions

needs special attention, since biomembrane systems are highly charged i.e. lipid molecules are either polar or charged and they interact with each other, the polar water environment, counterions (Pandit and Berkowitz *et al.*, 2002), proteins (Ibragimova and Wade *et al.*, 1998), and DNA (Bandyopadhyay *et al.*, 1999). Suitable handling of electrostatic interactions in MD simulations is therefore one of the most important issues in this field. In particular, the particle-mesh Ewald (PME) technique has been increasingly used often in lipid bilayer simulations to avoid such problems (Venable *et al.*, 2000; Saiz and Klein *et al.*, 2001; Feller *et al.*, 2002; Tobias *et al.*, 2001; Pandit and Berkowitz *et al.*, 2002).

1.8 Aims and Objectives

Membrane protein specific processes, pathways and interactions can't be characterized without knowing their interactions and placements in cell membrane. The basic aim of this study is to explore how connexin family proteins behave in lipid bilayer of cell membrane and to find the effect of T8M mutation in Cx26 i.e., how it behaves in plasma membrane that ultimately causes deafness. There is very little knowledge about MD simulations using Lipid-protein system and handling of lipid bilayer simulation is a difficult task. This study will largely help in establishing novel clues for Cx26 functional disturbances leading to non-syndromic deafness.

MATERIALS AND METHODS

2. Material and Methods

2.1 Data collection

Literature survey was performed to determine the causes of deafness. As 50% of Hearing loss is due to genetic abnormalities (Birkenhager *et al.*, 2007), genes involved in hearing were checked. Numerous genes were found to be affected in deafness. Out of these, Cx26 was selected for further analysis as rate of deafness caused by this gene was high as compared to other genes. As our study was focused on the deafness in Pakistan; so mutations of Cx26 frequently associated with deafness in Pakistani population were selected (Table 2.1).

Table 2.1: Cx26 mutations causing deafness in Pakistani families.

Mutation	Reference
p.T8M	Anjum *et al.*, 2014
p.W24R	Snoeckx *et al.*,2005
p.M34T	Kemperman *et al.*, 2002
c.167delT	Snoeckx *et al.*,2005
p.W24X	Kelsell *et al.*, 1997
p.R143W	Snoeckx *et al.*,2005
c.35delG	Carrasquillo *et al.*, 1997 Denoyelle *et al.*, 1997 Zelante *et al.*, 1997
p.W77X	Padma *et al.*, 2009

Among these mutations, T8M mutation is responsible for >6% cases of non-syndromic deafness in Pakistan (Anjum *et al.*, 2014).

2.2 Protein sequence and structure retrieval

Protein sequence of Cx26 was retrieved through Ensembl genome browser (Flicek *et al.*, 2011, Hubbard *et al.*, 2002) (*http://www.ensembl.org/index.html*), UCSC genome browser (Karolchik *et al.*, 2014, Fujita *et al.*, 2010) (*http://genome.ucsc.edu*) and Uniprot (*http://www.uniprot.org/*). Structure of Cx26 (PDB ID: 2ZW3) was obtained through Protein Data Bank (PDB) (Berman *et al.*, 2000) with 3.5Å resolution (Maeda *et al.*, 2009). This structure was employed for predicting the structures of mutated Cx26.

2.3 Structure prediction and minimization

Structure of mutated (T8M) Cx26 was predicted and minimized by Modeller9.14 (*http://salilab. org/modeller*). UCSF Chimera 1.8.1 (Goddard *et al.*, 2007) (*https://www.cgl.ucsf.edu/chimera/*) was used for structure visualization, sequence structure integration, structure minimization and 3D superimposition.

2.3.1 Modeller

Modeller is a program used to predict 3D models with good stereochemistry and close to crystallographic structure of template (Sali *et al.*, 1995). Modeller predicts 3D structure of a query protein (target) by aligning it with one or more proteins of known structures (templates). The steps of prediction process include: fold assignment, target-template alignment, model building, and model evaluation. Modeller is a comparative or homology based program, therefore errors may exist in case of no alignment between the query and template (Eswar *et al.*, 2006).

If sequence similarity between query and template is 40%, the predicted structure has about 90% of main chain atoms modeled with Root Mean Square Deviation from ~ 1Å resolution X-ray structure of template (Sali *et al.*, 1995, Eswar *et al.*, 2008).

2.3.2 UCSF Chimera

UCSF Chimera is an extensible interactive visualization tool for the analysis of molecular structures and related data. It provides easy analysis of sequence alignments, docking results, structural details. High-quality images and animations can also be generated (Pettersen *et al.*, 2004, Yang *et al.*, 2012). Chimera provides deep integration of sequence and structure, far beyond mapping where the primary sequence of protein falls in secondary

or tertiary structure. Thus sequence structure integration which was considered as a difficult task can be easily accomplished in Chimera. Chimera is used to superimpose structures so that they can be compared and analyzed (Meng *et al.*, 2006).

2.4 Structure validation and refinement

Validation of stereochemical properties of structures such as Ramachandran favoured residues, good and bad bonds and angles are checked by Molprobity and followed by refinement through Wincoot.

2.4.1 MolProbity

MolProbity (*http://molprobity.biochem.duke.edu/*) is a general-purpose web program which offers quality validations for three-dimensional (3D) structures of proteins, nucleic acids and complexes. It provides thorough analysis of all-atom contacts to find steric problems within the structures (Davis *et al.*, 2004). All diagnostics are presented in charts and graphical forms which help the researchers to make a quickly review structural details of proteins (Chen *et al.*, 2009). MolProbity is unique to the related programs in offering all-atom contact analysis and up-to-date, high-accuracy Ramachandran and rotamer distributions. MolProbity applies to both X-ray and NMR structures, and to both proteins and nucleic acids.

2.4.2 WinCoot

WinCoot is a molecular-graphics application which is utilized for model building and validation of biological structures. The program displays electron-density maps and atomic models (Emsley *et al.*, 2004). It allows model manipulations such as real-space refinement, manual rotation/translation, rigid-body fitting, ligand search, solvation, mutations, rotamers and Ramachandran idealization (Emsley *et al.*, 2010). WinCoot helps in refining the structures such as poor rotamers, ramachandran outliers etc. are removed. WinCoot is built around two major libraries: mmdb (A library for handling molecular macromolecules) and clipper (Cowtan *et al.*, 2002).

2.4.3 YASARA

YASARA is a modeling, minimization and dynamics program built around the visualization algorithm (Krieger *et al.*, 2014). YASARA features a complete homology

modeling module to automatically generate a high-resolution model using a CASP (Critical Assessment of Structure Prediction) approved protocol (Krieger *et al.*, 2009). It is powerful enough to handle large amounts of data produced in structural and functional proteomic projects i.e. all-in-one solution to map protein sequence onto 3D structure. The functional annotation of proteins ultimately aids the process of drug designing. YASARA is a platform to perform flexible ligand-receptor dockings as well as short simulations.

2.5 Visualization and analysis

Visualization of the interaction of docked and simulated complexes is done with LigPlus (*http://www.ebi.ac.uk/thornton-srv/software/LigPlus/*) and Pymol (*http://pymol.org/educational/*), TmRPres2D (*http://bioinformatics.biol.uoa.gr/TMRPres2D/*) is used to visualize Cx26 in membrane. Caver is used to calculate pore size of normal and mutated (T8M) Cx26, to determine the influence of pore size in causing deafness.

2.5.1 TmRPres2D

TmRPres2D is the abbreviation of "Transmembrane Re-presentation in 2D". It is a java based application which takes protein sequence as input and presentsuniform and two-dimensional high quality graphical models of alpha-helical or beta-barrel regions of transmembrane proteins (Spyropoulos *et al.*, 2004).

2.5.2 Caver

Caver is a downloadable program developed in JAVA which serves to identify transport pathways of macromolecules. It can be used either as PyMol plugin or independent application. It not only predicts tunnel locations in protein structures but also supports their analysis and calculation, real-time visualization of tunnels and channels (Kozlikova *et al.*, 2014). A trajectory from a molecular dynamics simulation serves as the typical input (Chovancova *et al.*, 2012). Other than protein system caver is able to analyze any molecular system i.e. nucleic acids or inorganic material (Petrek *et al.*, 2006)

2.5.3 LigPlus

LigPlus is an intuitive java interface which allows on-screen editing of the plots via mouse click-and-drag operations. This application generates two dimensional (2D) protein-ligand

interaction diagrams from 3D coordinate files. Using this program, hydrogen and hydrophobic interactions between ligands and amino acid residues within the active site can be analyzed (Wallace *et al.*, 1995). To facilitate interaction analysis of multiple ligands within the same protein, the application is now able to plot all related sets of ligand-protein interactions in the same orientation (Laskowski *et al.*, 2011).

2.5.4 Pymol

Pymol (*http://pymol.org/educational/*) is an open-source and user-sponsored molecular visualization system created by Warren Lyford DeLano and commercialized by DeLano Scientific LLC. It can produce high-quality 3D images of small molecules and biological macromolecules, such as proteins. It is one of the few open-source visualization tools available for use in structural biology. Almost a quarter of all published images of 3D protein structures in the scientific literature are created in Pymol. It is used for 3D visualization of proteins, small molecules, molecular surfaces, and simulation trajectories. It also includes functions such as molecular editing (Baugh *et al.*, 2011).

2.6 Molecular dynamics simulation assays

Gromacs 4.5.5 with Gromos93a6 force field was used for simulating the wild type and mutated Cx26 in lipid bilayer i.e., Dipalmitoylphosphatidylcholine (DPPC). RMSD, Radius of gyration, RMSF, hydrogen bonds and energy plots were generated by GROMACS tools to check the quality of simulations.

2.6.1 GROMACS

Molecular dynamics (MD) is a computer simulation technique that allows one to predict the time evolution of a system of interacting particles. MD simulations are based on classic mechanics laws and Newton's laws of motion. GROMACS (Groningen MAchine for Chemical Simulation) was developed at the University of Groningen, in the early 1990s. It is fast, flexible and free server for simulation of real world processes (Berendsen *et al.*, 1995, Van Der Spoel *et al.*, 2005, Hess *et al.*, 2008, Pronk *et al.*, 2013). It is compatible with a variety of force fields such as GROMOS, OPLS, AMBER, and ENCAD.

2.6.1.1 Preparation of PDB files

Some residues or atoms may be damaged during minimization; therefore PDB files were checked for missing residues and repaired by AutoDock before running molecular dynamics simulations.

2.6.1.2 Topology building

Topology coordinates were generated by GROMACS pdb2gmx commands. The files contain force field parameters and information about the composition of the artificial system to be created.

2.6.1.3 Periodic box generation and pack the lipid around protein

Water model for salvation is selected. In our case we used SPC216 as it suited our system. Protein and membrane were oriented in a cubic periodic box and then lipids were packed around the protein.

2.6.1.4 System neutralization

Neutralization of overall system is important, therefore charge on the system was calculated and ions were added to neutralize the system.

2.6.1.5 Energy minimization

Energy minimization of the system was performed to determine the lowest energy. In total, 50,000 steps were run through steepest descent algorithm.

2.6.1.6 Equilibration

For membrane protein simulations, we created special index groups consisting of solvent + ions and protein + lipids. Then system was equilibrated for 10000 ps at constant temperature (300K) and pressure (1 ATM) with hydrogen bond length constraints for numerical integration with leap-frog algorithm. NVT and NPT equilibration phase is important for stabilizing the temperature and pressure of the system (Yu *et al.*, 2012).

2.6.1.7 MD simulation run

Finally, after completion of equilibration phase MD simulation runs were performed for 10ns time scale under constant temperature and pressure. PME (Particle Mesh Ewald) algorithm was used for all calculations.

2.6.1.8 Trajectory Analysis

After the completion of molecular dynamics simulations we wanted to analyze how our protein behaved in the course of time; therefore analysis of various dimensions (RMSF, RMSD, Radius of Gyration, hydrogen bonds, energy, and interaction analysis) was performed. To analyse conformational changes, PDB files at time scale 1, 3, 6 and 9 ns for protein as well as lipid were generated to determine their interaction.

2.7 Work Strategy

Work flow of whole process that has been followed during research is given in figure 2.1.

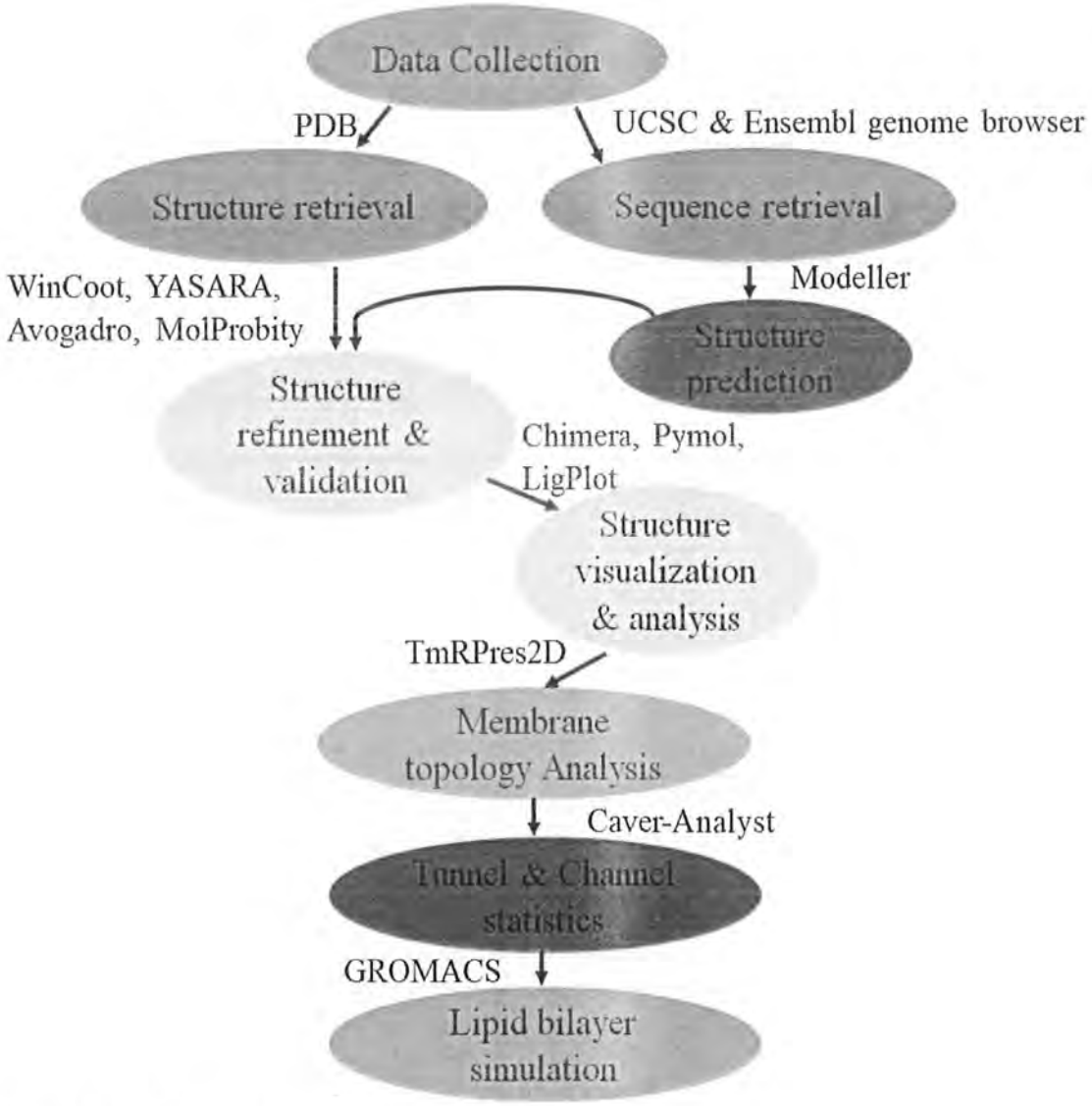

Figure 2.1: Primary steps followed in research project.

RESULTS

3. Results

3.1 Structure Prediction

Mutated structure for T8M ($Cx26^{MUT}$) was predicted by mutating the residue T8 into M using the $Cx26^{WT}$ as reference structure. $Cx26^{MUT}$ structures were verified by Molprobity results for steriochemical properties such as Ramachandran plot, Ramachandran outlier and bad bonds etc.These Molprobity results were compared with reference $Cx26^{WT}$ structure results to confirm valid prediction. Molprobity results for $Cx26^{WT}$ and $Cx26^{MUT}$ were given in Table 3.1 and Table 3.2 respectively.

Table 3.1: Molprobity results of $Cx26^{WT}$.

Favoured Rotamers	733	67.87%
Poor Rotamers	153	14.17%
Ramachandran favoured	1100	93.06%
Ramachandran outliers	6	0.51%
Bad angles	0/10170	0.00%
Bad bonds	133/13818	0.96%

Table 3.2: Molprobity results of $Cx26^{MUT}$.

Favoured Rotamers	1032	84.31%
Poor Rotamers	78	6.37%
Ramachandran favoured	1094	91.5%
Ramachandran outliers	8	0.60%
Bad angles	44/13818	0.3%
Bad bonds	2/10170	0.019%

3.2 Structure Analysis

Structure of Cx26 hexamer is a simple arrangement of six chains in which each chain is composed of four transmembrane helices (TM1-TM4), two cytoplasmic loops and an extracellular loop. Both wild type and mutated 2-dimemnsion (2D) structures were compared. 2D structure comparison was given in Figure 3.1. Evidently, some α-helices changed their conformations and β-sheets were smaller and less in number in $Cx26^{MUT}$. To confirm these alterations, 3-dimension (3D) structures of both $Cx26^{WT}$ and $Cx26^{MUT}$ were

superimposed. An RMSD value of 0.450Å was observed. 3D structure of $Cx26^{MUT}$ was scattered and disorganized, while $Cx26^{WT}$ was compact as shown in Figure 3.2. 1st transmembrane α-helix was 30 residue long (21 – 50 AA) in $Cx26^{WT}$ structure, while in $Cx26^{MUT}$, there was a helix break occurred in 1st α-helix at Trp44. In $Cx26^{MUT}$ structure, two α-helices (from 20 – 43 AA and 45 – 49 AA) were detected compared to one helix in $Cx26^{WT}$. In $Cx26^{WT}$ structure, Val52-Cys53 residues were located in β-sheet which was absent in $Cx26^{MUT}$ structure. An α-helix present at residue Ser72-Phe106 in $Cx26^{WT}$ was shifted at Ile73-Ile107 residues in $Cx26^{MUT}$ structure. Another α-helix was a little bit longer in $Cx26^{MUT}$ structure from Val126 – Val156 AA as compared to $Cx26^{WT}$ where it was from Gly130 -Met157 AA. Two β-sheets were present exactly at same locations in both structures (1st β-sheet at residue Leu166-Cys169 and 2nd at Val178 to Phe181). Last α-helix was present at residue Arg184-Arg216 in $Cx26^{WT}$ and at residue Pro185-Arg216 in $Cx26^{MUT}$ structure. Thus T8M mutation resulted in a lot of structural changes leading to functional disturbance.

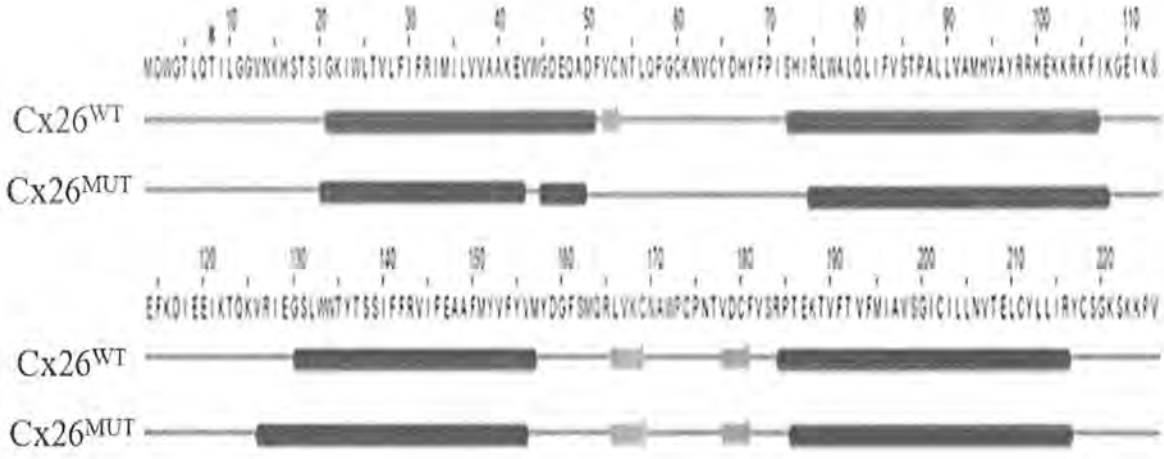

Figure 3.1: 2D structure of $Cx26^{WT}$ and $Cx26^{MUT}$. Red rectangles show α-helices, green arrows represent β-sheets and solid lines show loops in both structures. Arrow indicates the position of mutated residue.

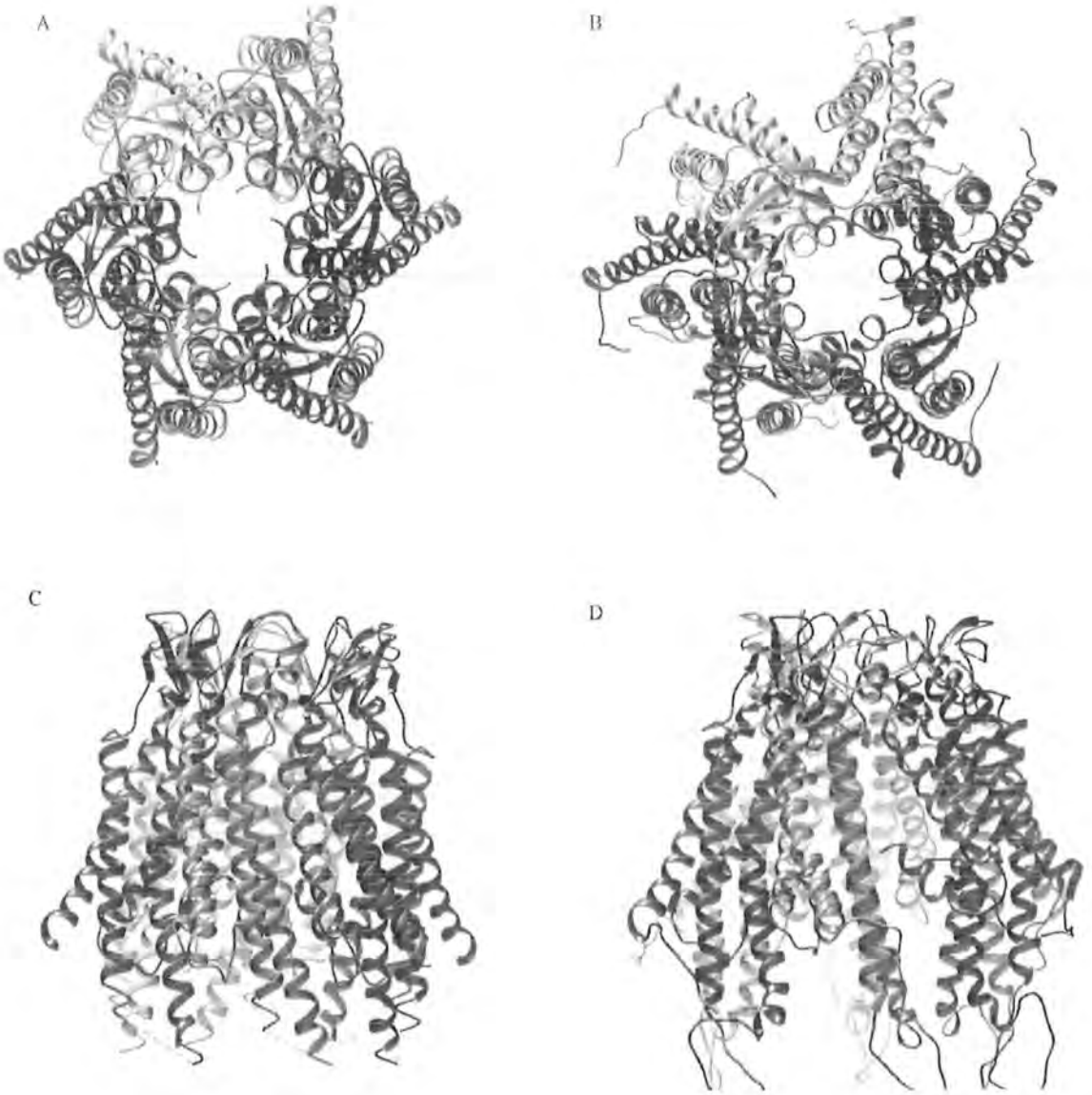

Figure 3.2: Ribbon representation of $Cx26^{WT}$ and $Cx26^{MUT}$ 3D structures. A and B shows front view, while C and D shows side view of structures.

3.3 Topology analysis

Membrane topology of α-helices plays an important role in proper functioning of membrane proteins. $Cx26^{WT}$ exhibited two cytoplasmic loops and one extracellular loop, while it was located at opposite orientation in $Cx26^{MUT}$ which contained two extracellular loop and one cytoplasmic loop (Figure 3.3). C-terminus of $Cx26^{WT}$ was located in the extracellular region, while in $Cx26^{MUT}$, it was adjusted in cytoplasmic region. Helical positions with in membrane, cytoplasmic and extracellular regions were different between two structures. $Cx26^{WT}$ exhibited four transmembrane helices in an organized arrangement. In case of $Cx26^{MUT}$, 1st α-helix had a break which caused disturbance in transmembrane helical arrangements. Placement of transmembrane helices in plasma membrane for $Cx26^{WT}$ and $Cx26^{MUT}$ was shown in Figure 3.3.

3.4 Pore and tunnel statistics

Membrane proteins have cavities or pores and form intercellular tunnels for the passage of 2nd messengers (ions and small molecules) between adjacent cells. This intercellular transportation is important for proper body functioning. Cx26 is a hexamer membrane protein and has a pore in the form of tunnel for the passage of 2nd messengers. Pore diameter measured for $Cx26^{WT}$ was 21.5Å (Figure 3.4) which was shorten in case of $Cx26^{MUT}$ due to conformational alterations that caused disturbance in whole structure. Pore diameter measured for $Cx26^{MUT}$ was 12Å (Figure 3.4). Area of pore measured for $Cx26^{WT}$ was 363Å^2, while it was 113Å^2 for $Cx26^{MUT}$ (Figure 3.5).

Cx26 pore leads to a tunnel for passage of ions (Ca^{2+} and K^+) and small molecules (IP3) between cells. Length of tunnel for $Cx26^{WT}$ was 17.128Å while for $Cx26^{MUT}$ it was 14.4Å (Figure 3.7). A drastic shortening of tunnel occurred in $Cx26^{MUT}$ (Figure 3.6) due to T8M mutation. Tunnel statistics comparison was given in table 3.3.

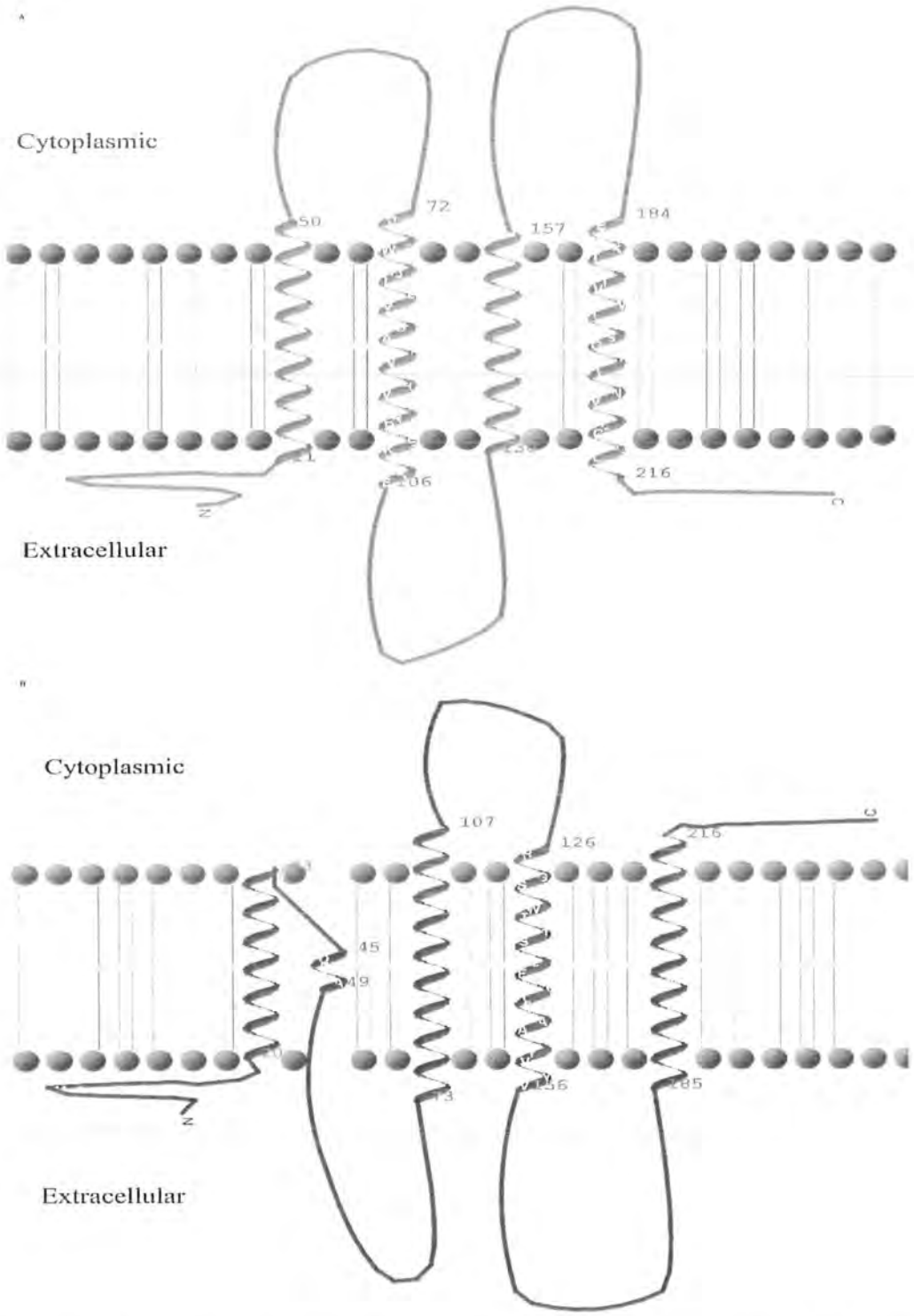

Figure 3.3: Membrane topology of transmembrane helices of $Cx26^{WT}$ and $Cx26^{MUT}$. Green part represents topology of $Cx26^{WT}$ structure, while red color shows topology of $Cx26^{MUT}$ structure.

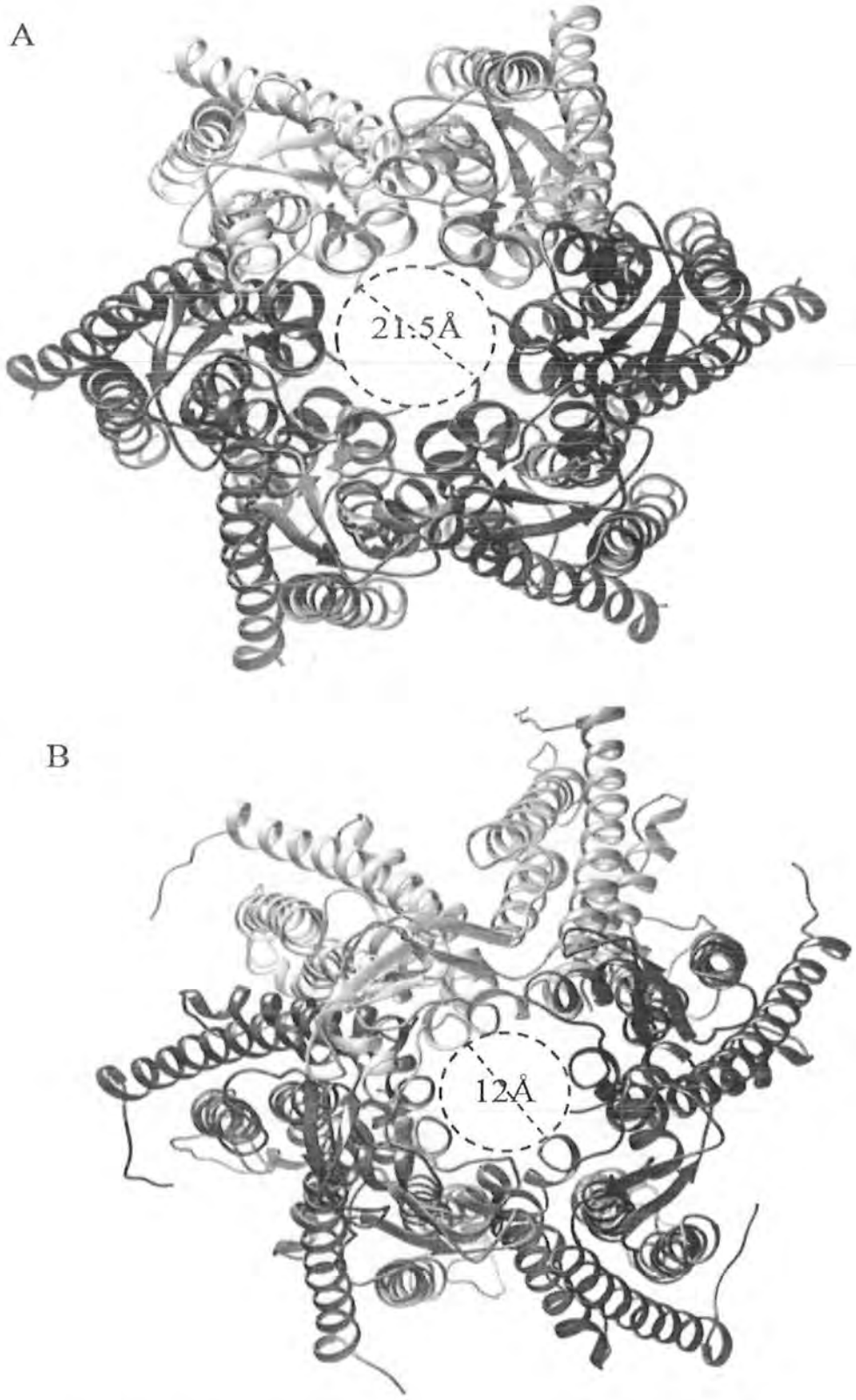

Figure 3.4: Pore diameters of wild-type (A) and mutated (B) Cx26.

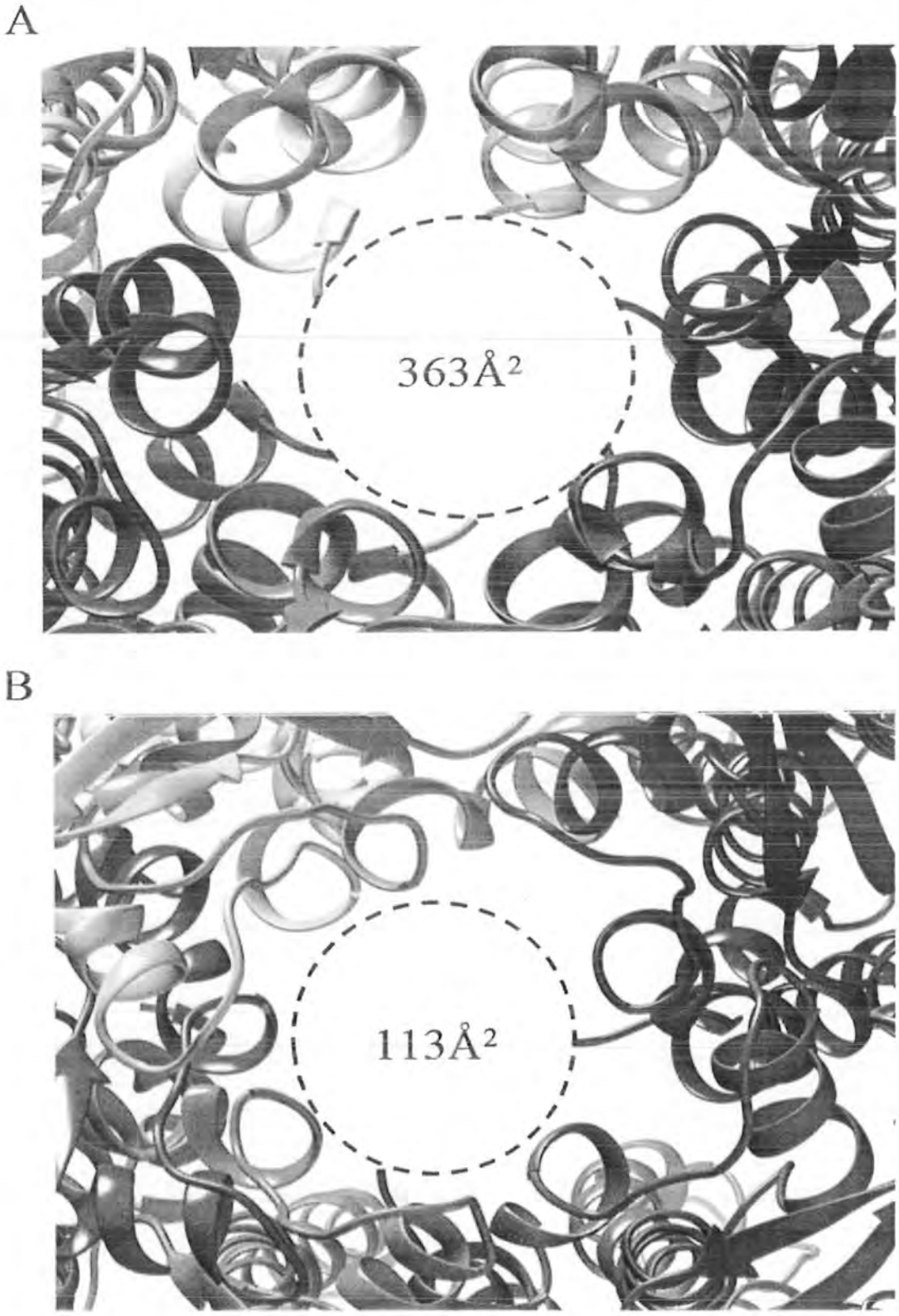

Figure 3.5: Area representation for wild-type (A) and mutated (B) Cx26 structures.

Table 3.3: Tunnel statistical analysis of $Cx26^{WT}$ and $Cx26^{MUT}$ structures. In this table Avg_BR [Å] (average bottleneck radius). Max_BR [Å] (maximum bottleneck radius). Avg_L [Å] (average channel length). Avg_C (average channel curvature).

Properties	$Cx26^{WT}$	$Cx26^{MUT}$
Avg_BR [Å]	10.772	6.817
Max_BR [Å]	10.77	6.82
Avg_L [Å]	17.128	14.4
Avg_C	1.24	1.142

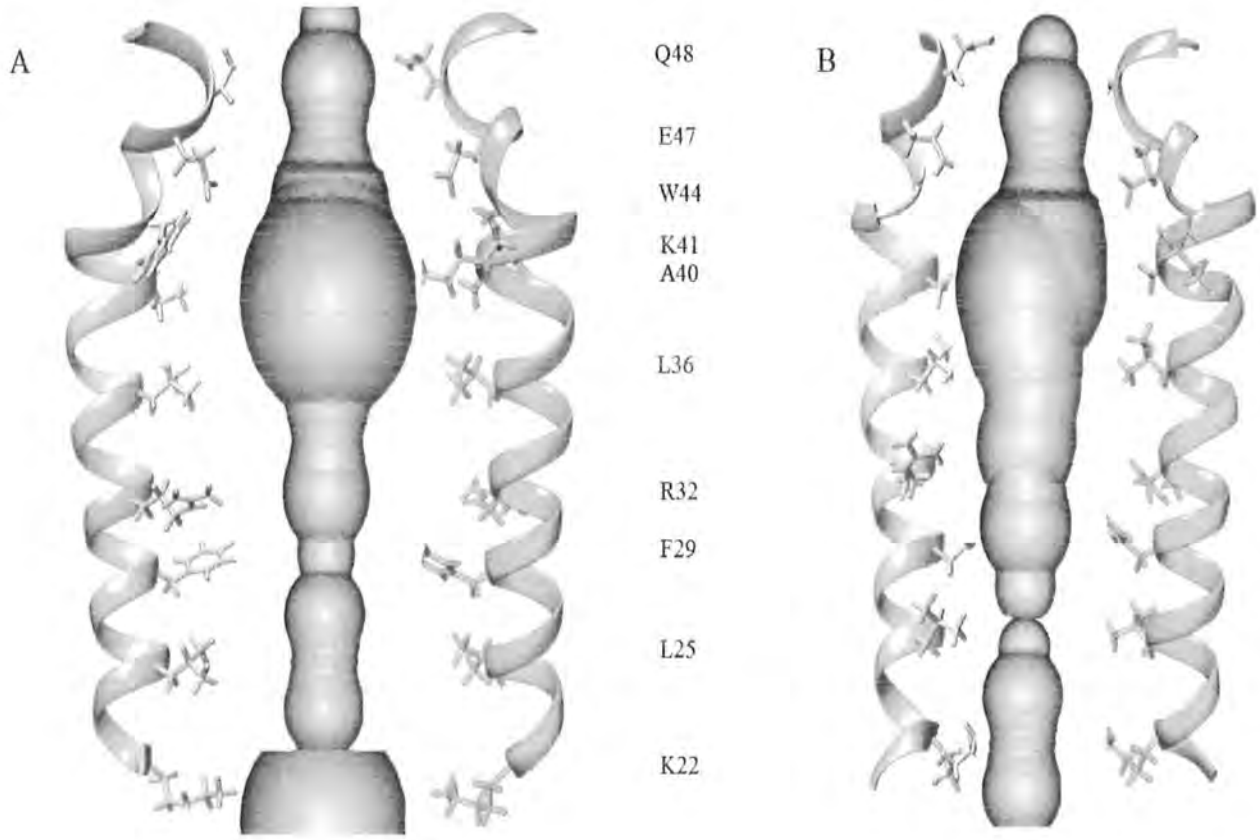

Figure 3.6: Tunnel representation in $Cx26^{WT}$ (A) and $Cx26^{MUT}$ (B) structures.

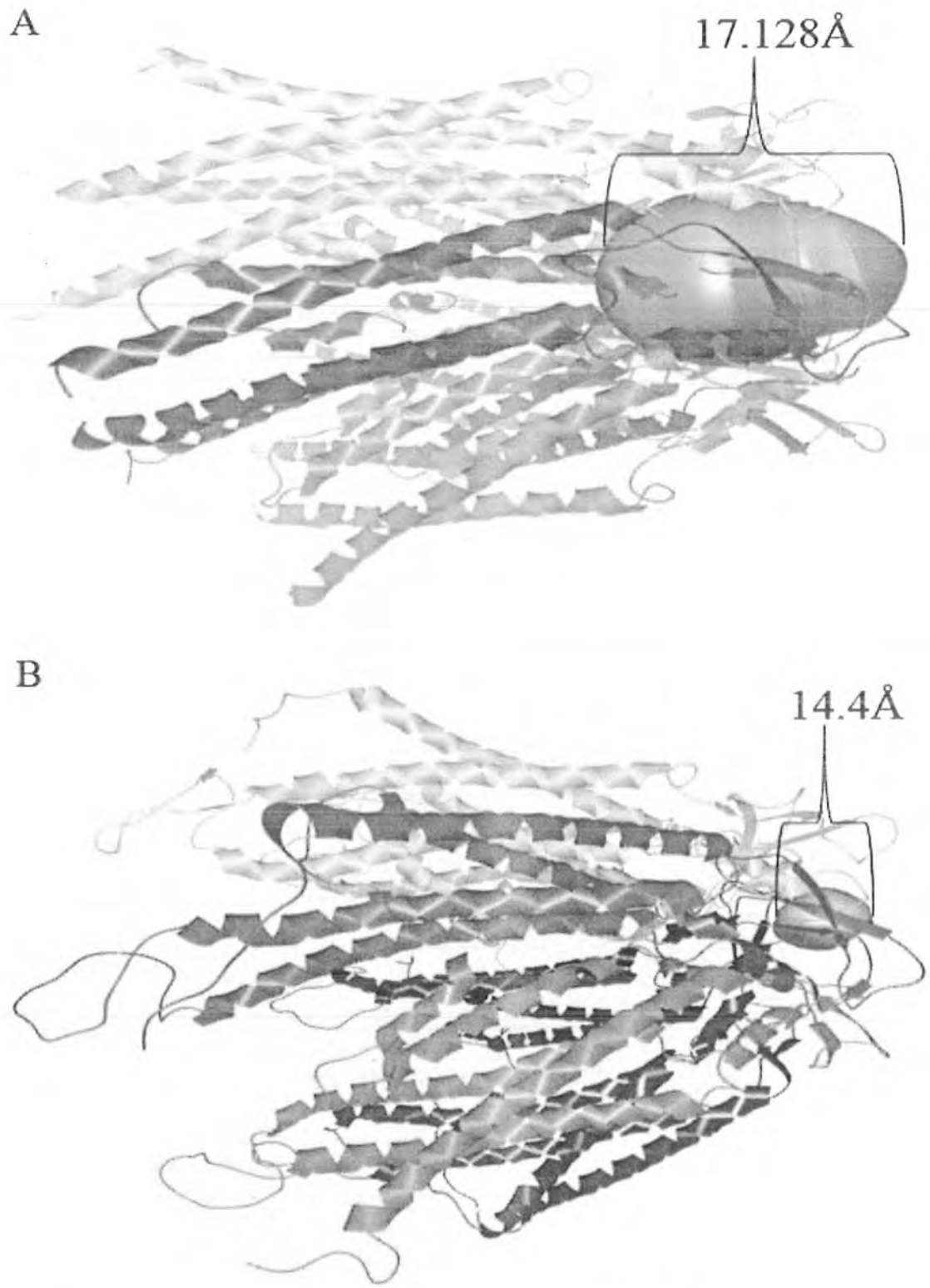

Figure 3.7: Side view of $Cx26^{WT}$ (A) and $Cx26^{MUT}$ (B) Tunnel.

3.5 Lipid bilayer simulation Analysis

Study of membrane proteins like Cx26 with lipids is of structural and functional significance. In order to check the overall protein stability and time-dependent interactions with membrane lipids, MD simulations of $Cx26^{WT}$ and $Cx26^{MUT}$ with in lipid bilayer of Dipalmitoylphosphatidylcholine (DPPC) were performed for 10 ns. Resulting trajectories were carefully analysed to determine stability, convergence, interactions, energetics and structural properties during MD simulations. To evaluate the stability and fluctuations of $Cx26^{WT}$ and $Cx26^{MUT}$ with in DPPC, time series of root mean square deviation (RMSD), root mean square fluctuation (RMSF) and radius of gyration (Rg) were generated.

RMSD profiles for both $Cx26^{WT}$-DPPC and $Cx26^{MUT}$-DPPC were calculated with unbound $Cx26^{WT}$ state as a reference. Average RMSD for C-alpha atoms of overall system was below 3.5Å while for DPPC system, it was 1Å (Figure 3.8). RMSD plot showed that DPPC interactions resulted in the stabilization of protein, as it remained stable throughout simulations.

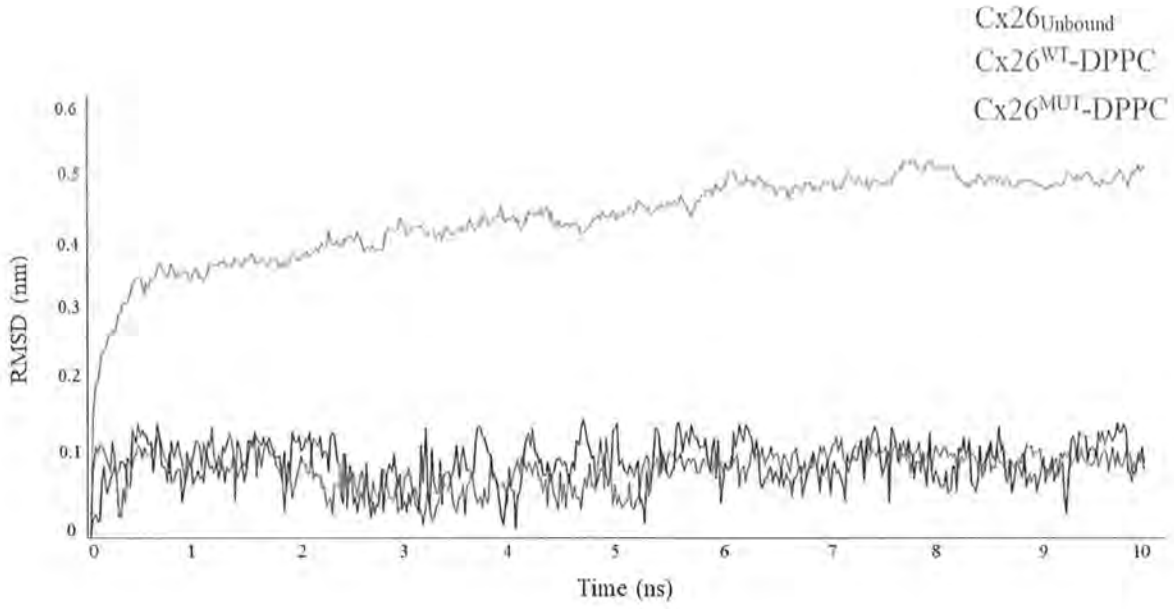

Figure 3.8: RMSD of $Cx26^{WT}$-unbound, $Cx26^{WT}$-DPPC and $Cx26^{MUT}$-DPPC systems.

Radius of gyration (Rg) is degree of stability and compactness of the system and gradually inclines to change over time due to protein folded-unfolded states. Rg plot for $Cx26^{WT}$ without lipid system showed that the system was unstable at start (deviation upto 2.7Å), while later on, it started to get stabilize and the protein was stabilized at 1ns (Figure 3.9). For $Cx26^{WT}$ and $Cx26^{MUT}$ in DPPC system, Rg curves were throughout stable from 1 ns as shown in Figure 3.10. Rg plots for the systems were consistent with their corresponding RMSD plots.

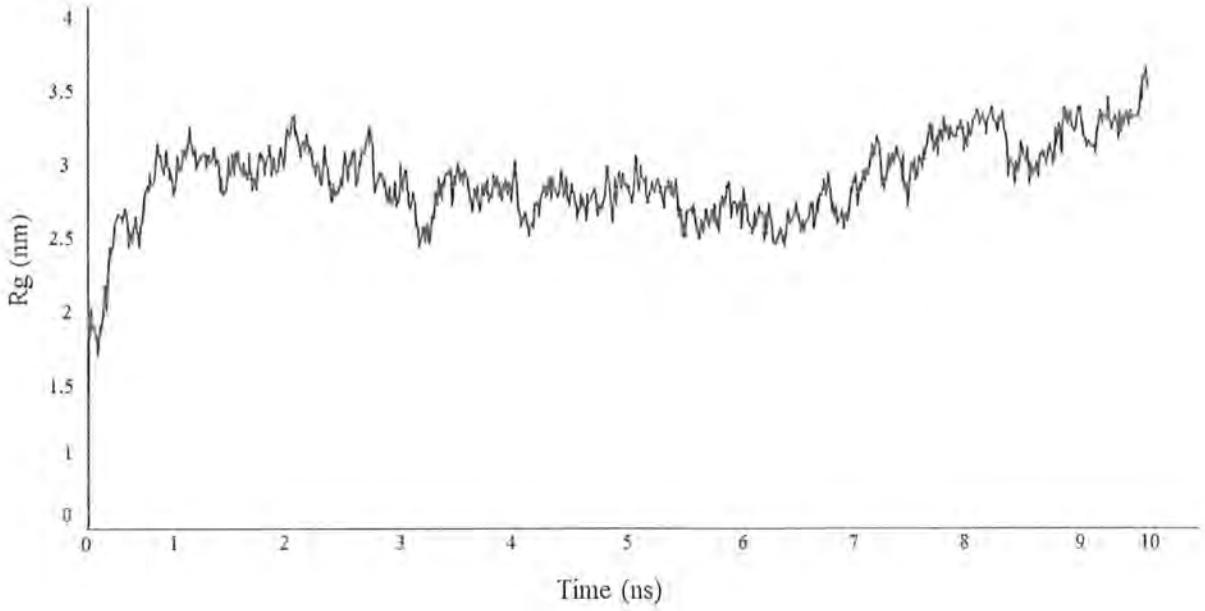

Figure 3.9: Rg plot of $Cx26^{WT}$-Unbound.

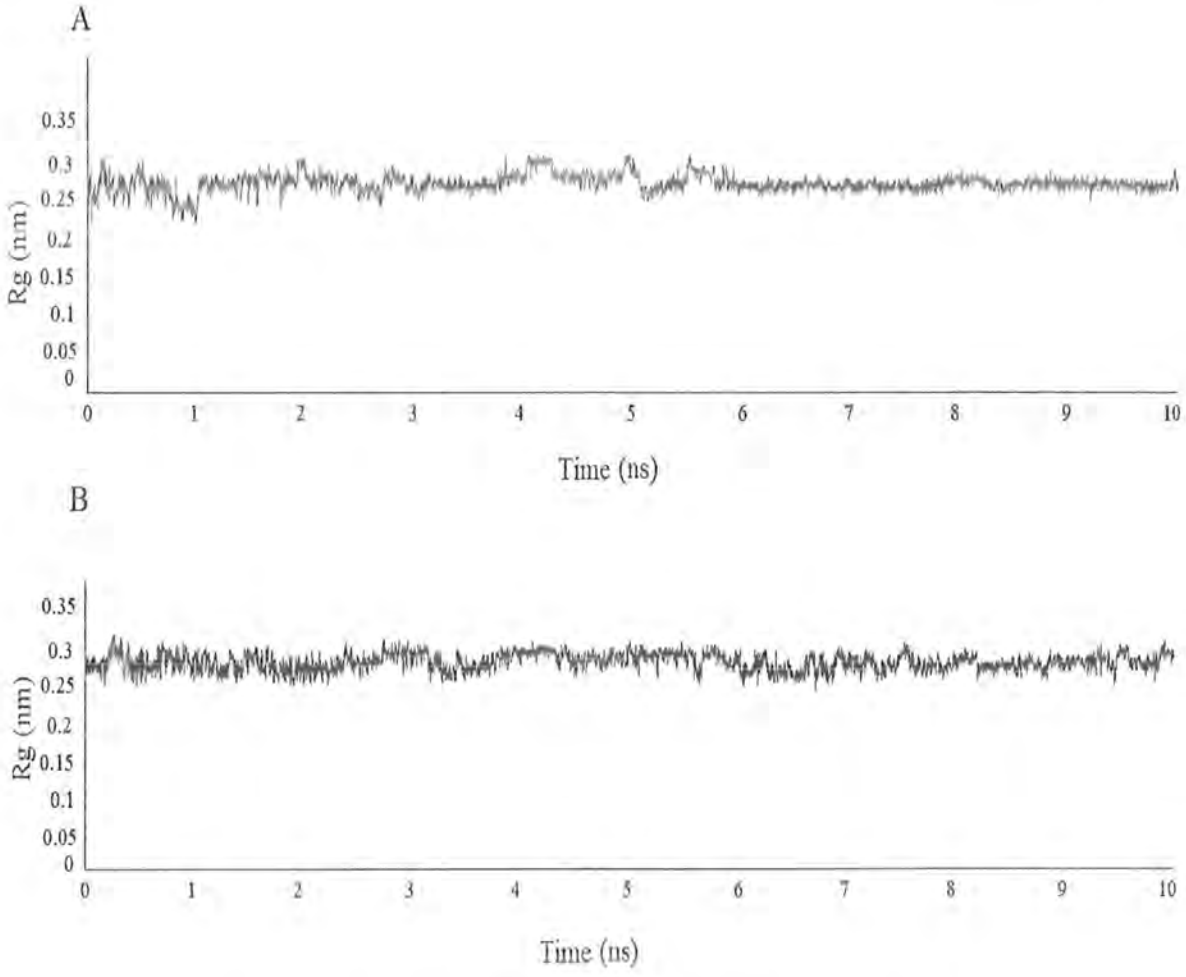

Figure 3.10: Rg plots of $Cx26^{WT}$ and $Cx26^{MUT}$ with in DPPC lipid bilayer system. A shows plot for $Cx26^{WT}$, while B shows plot for $Cx26^{MUT}$.

Analysis of RMSF indicated that fluctuations were observed in both $Cx26^{WT}$ and $Cx26^{MUT}$. Most of fluctuations were in the loop regions, while the helix region remained stable. Gly12-Asn14, Thr18-Ile20 and Ile107-Gly109 showed major fluctuations (Figure 3.11). RMSF for DPPC during MD simulation demonstrated that lipid bilayer (DPPC) also exhibited fluctuations. DPP79-DPP81, DPP4, DPP6, DPP101-DPP105, DPP110-DPP-112 and DPP126 showed major fluctuations (Figure 3.12).

During MD simulations, interactions of both proteins at different time intervals were determined to observe connections of both proteins with lipid bilayer system. In lipid bilayer environment, positions of both $Cx26^{WT}$ and $Cx26^{MUT}$ remained same, however, there were significant differences in interaction of these two structures with lipid bilayer of cell membrane. Details of hydrogen bonding interaction with DPPC were given in Table 3.4 and Table 3.5. Position of proteins within lipid (DPPC) was shown in Figure 3.13 and interactions were shown in Figure 3.14.

T8M mutation in Cx26 changed interactions with other helices and the lipid bilayer that correlated with decreased functionality. This prevented Cx26 interaction with 2nd messenger i.e. IP3 that resulted in low concentration of Ca^{2+} ions through pore of $Cx26^{MUT}$ (Figure 3.15). These Ca^{2+} ions were compulsory to keep balance of K^{+} ions (necessary for sound generation). Inhibition of IP3 interaction with Cx26 along with low concentration of Ca^{2+} ions ultimately caused non-syndromic deafness.

Table 3.4: DPPC bonding with $Cx26^{WT}$.

Lipid name	Hydrongen bond length (Å)
DPP-5	1.9
DPP-7	1.7
DPP-8	1.6
DPP-9	2.2
DPP-11	1.9
DPP-12	2.7
DPP-15	2.0

DPP-16	2.3
DPP-22	2.5
DPP-29	1.6
DPP-67	1.8
DPP-75	1.7
DPP-76	3.2
DPP-77	3.1
DPP-80	3.3
DPP-100	1.5

Table 3.5: DPPC bonding with $Cx26^{MUT}$.

Lipid name	Hydrongen bond length (Å)
DPP-5	1.6
DPP-8	2.2
DPP-9	1.9
DPP-12	2.7
DPP-15	2.0
DPP-16	2.3
DPP-22	2.5
DPP-23	1.6
DPP-26	1.8
DPP-29	1.7
DPP-47	3.2
DPP-65	3.1
DPP-76	3.3

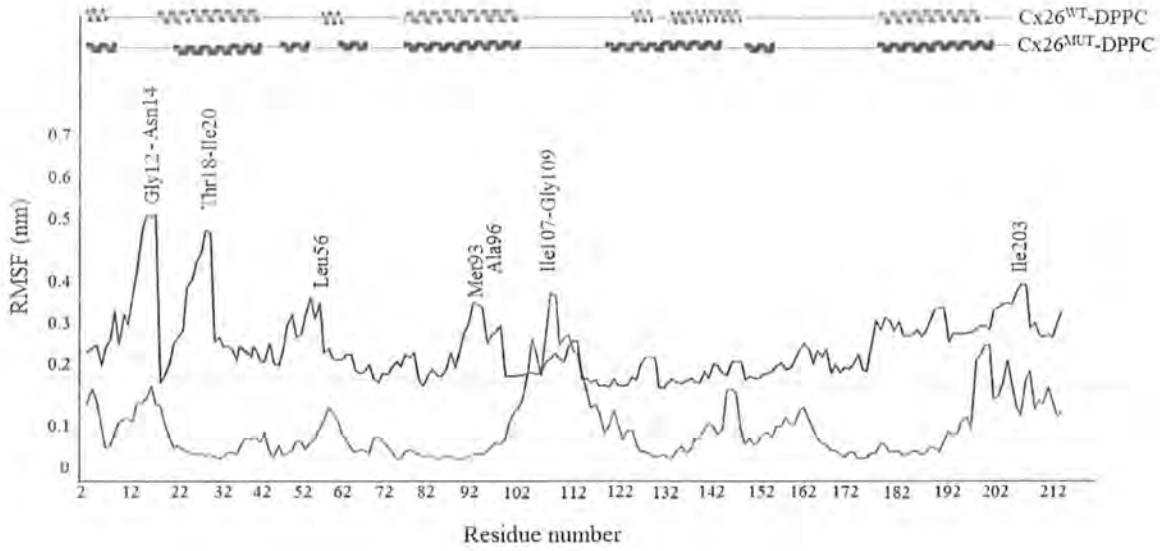

Figure 3.11: RMSF of $Cx26^{WT}$ and $Cx26^{MUT}$ with in DPPC lipid bilayer system. Green solid line shows $Cx26^{WT}$, while red solid line shows $Cx26^{MUT}$.

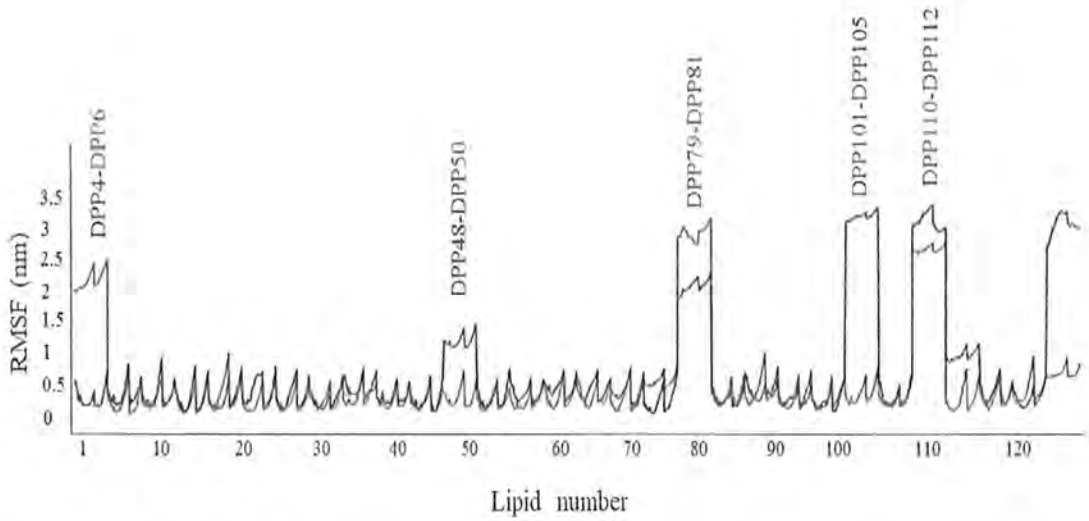

Figure 3.12: RMSF of DPPC lipid bilayer. Green solid line shows DPPC layer with $Cx26^{WT}$, while red solid line shows $Cx26^{MUT}$.

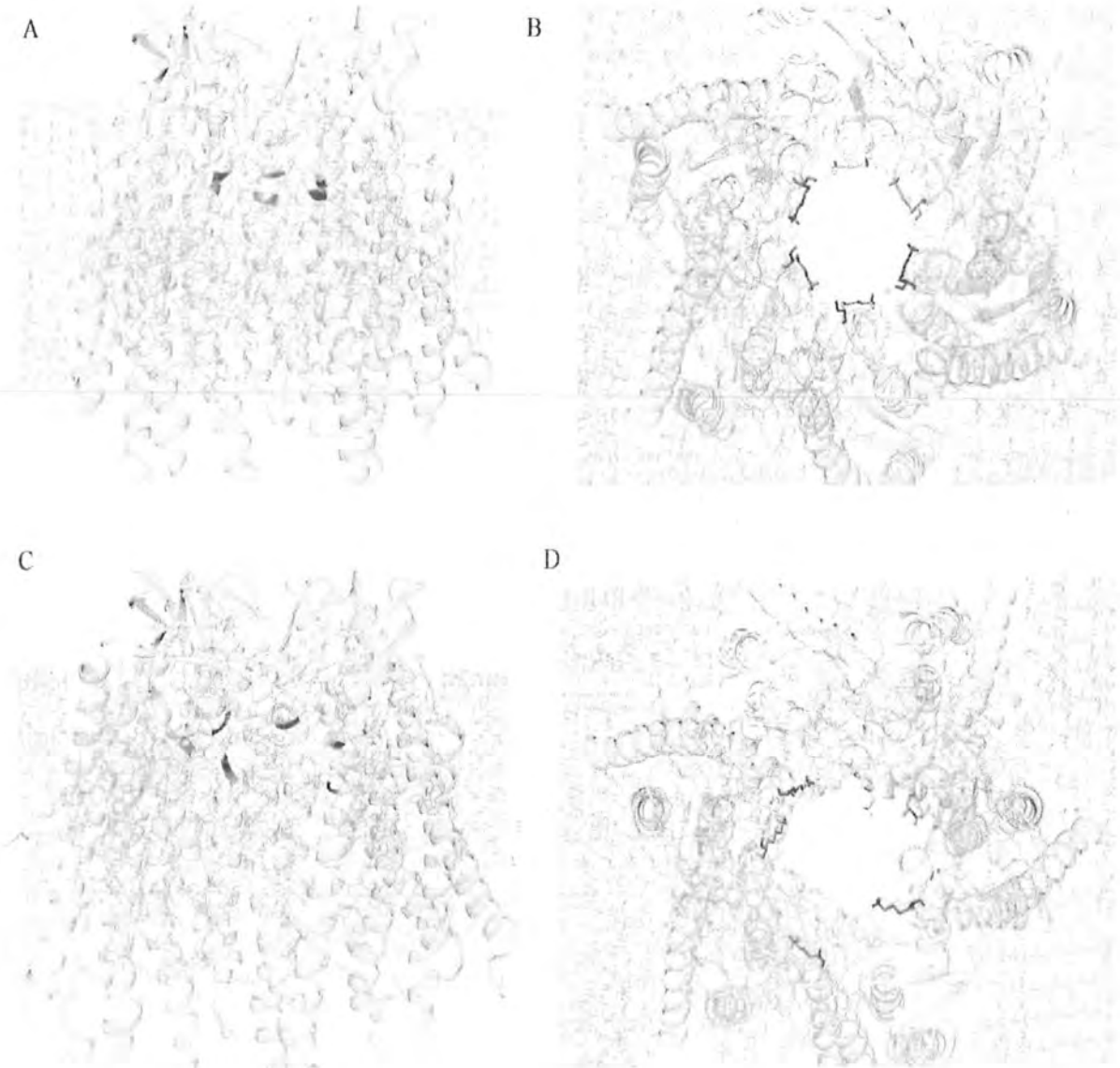

Figure 3.13: $Cx26^{WT}$ and $Cx26^{MUT}$ positions with in lipid bilayer system. A and B show $Cx26^{WT}$ side view and front view, respectively. C and D show $Cx26^{MUT}$ side view and front view, respectively.

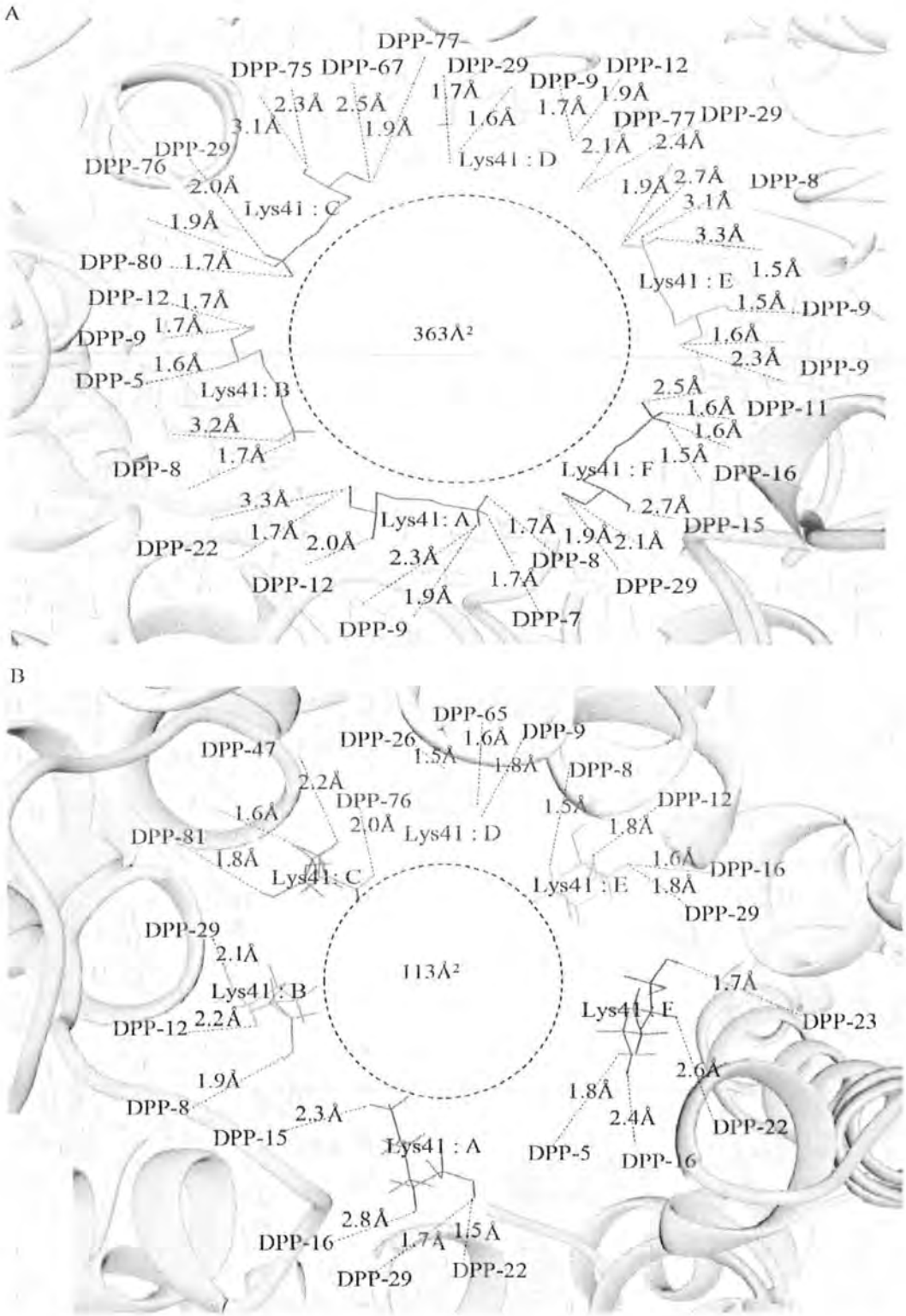

Figure 3.14: Cx26^{WT} and Cx26^{MUT} interactions with DPPC lipid bilayer. A and B shows Cx26^{WT} and Cx26^{MUT}, respectively.

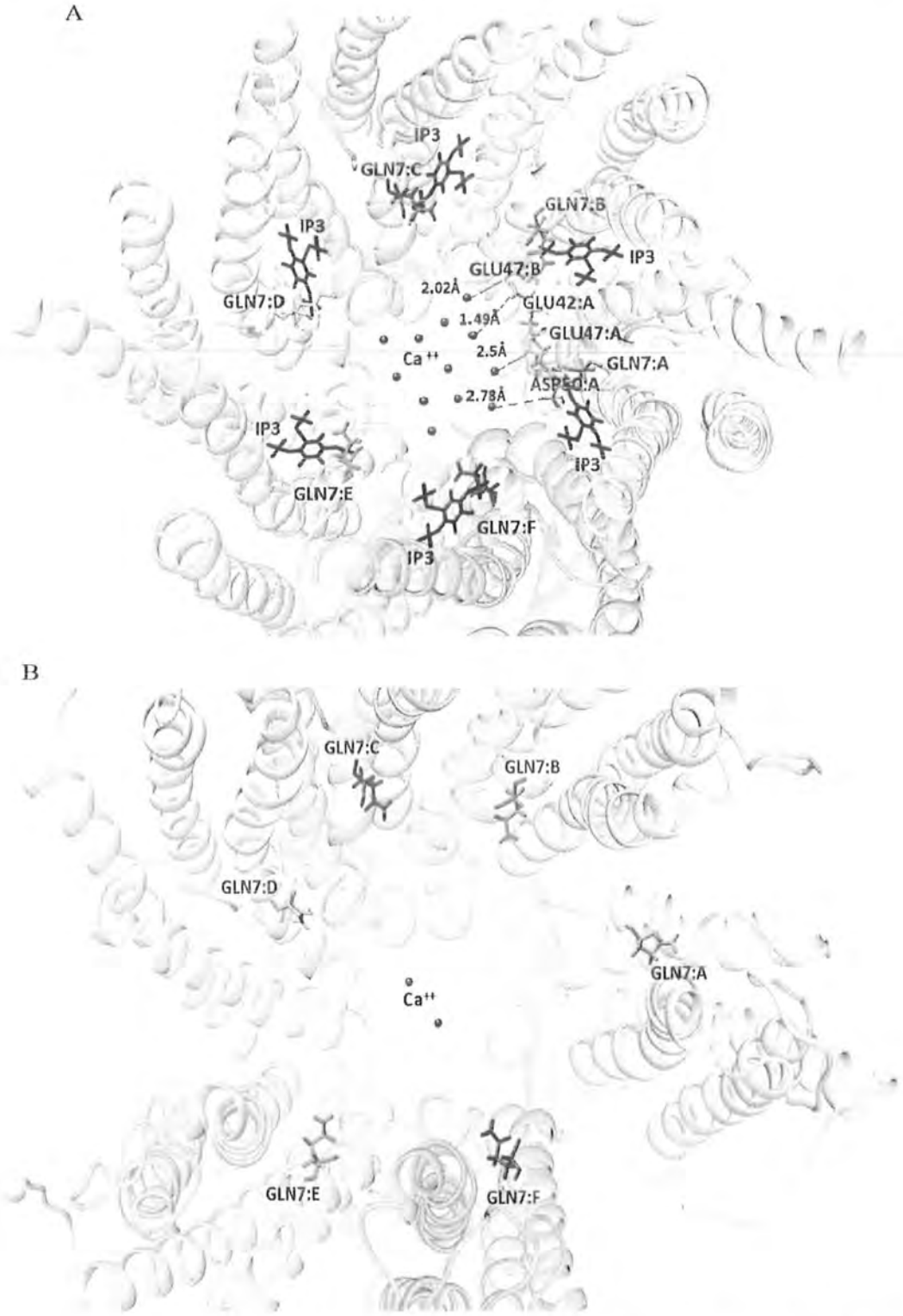

Figure 3.15: Passage of 2nd messengers (Ca^{2+} ions and IP3) through $Cx26^{WT}$ (A) and $Cx26^{MUT}$ (B).

The binding characteristics of $Cx26^{WT}$ and $Cx26^{MUT}$ with DPPC were analyzed through plotting time-dependent intermolecular hydrogen bonds. In $Cx26^{MUT}$-DPPC system binding was increased after 1.5 ns but overall $Cx26^{WT}$-DPPC system exhibited higher number of bonds as compared to $Cx26^{MUT}$-DPPC system. These results verified that $Cx26^{WT}$ exhibited more stable binding to DPPC compared to $Cx26^{MUT}$ (Figure 3.16).

The potential energy of a system is measure of its stability. By plotting potential energy as a function of time, we observed that systems were well equilibrated and remained stable throughout MD simulations. The $Cx26^{WT}$-DPPC (-328000 kcal/mol) system had showed lower potential energy value as compared to $Cx26^{MUT}$-DPPC (-326000kcal/mol) complex (Figure 3.17).

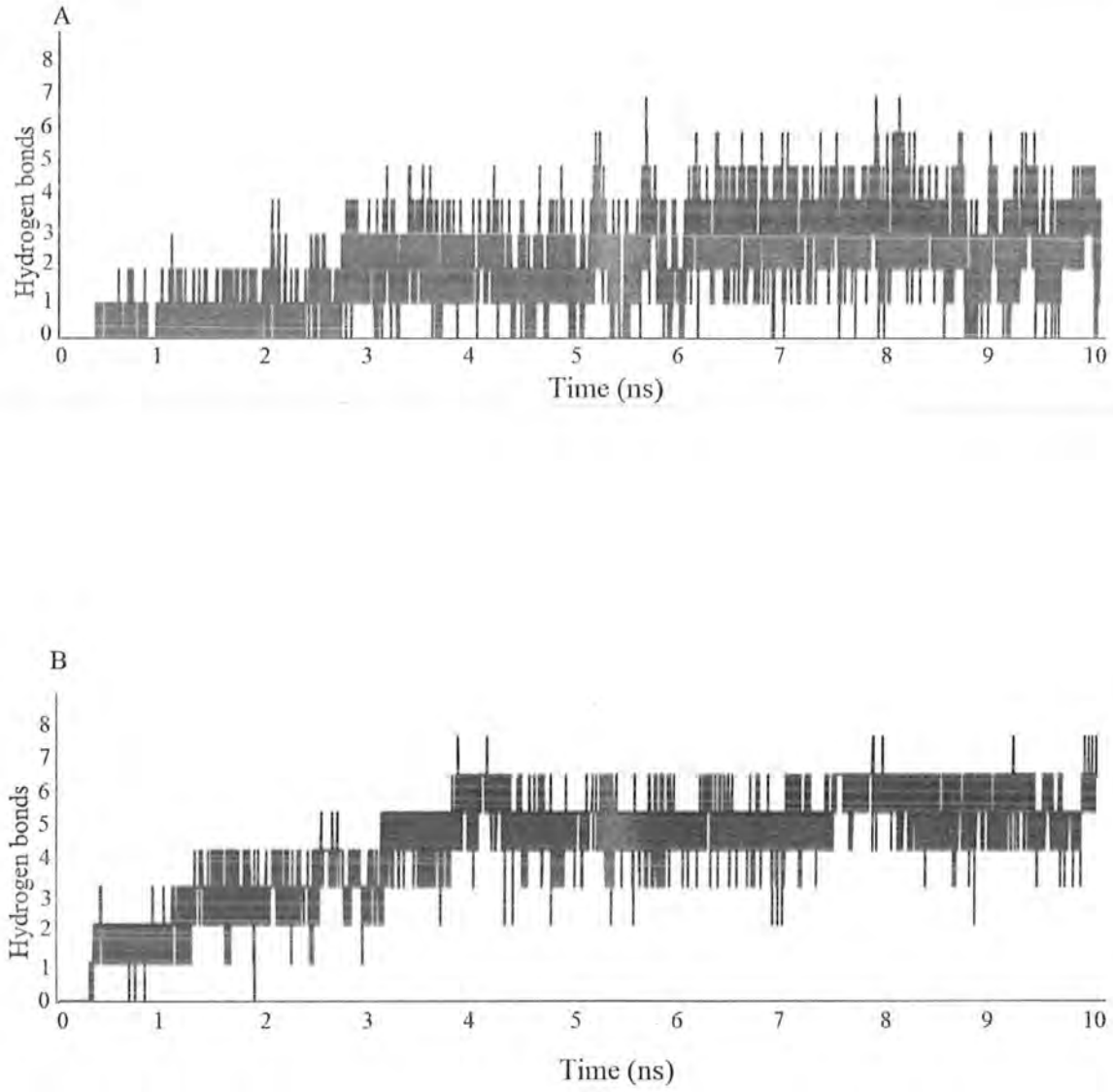

Figure 3.16: Hydrogen bond plot. A shows $CX26^{WT}$-DPPC interactions, while B shows $CX26^{MUT}$-DPPC interactions.

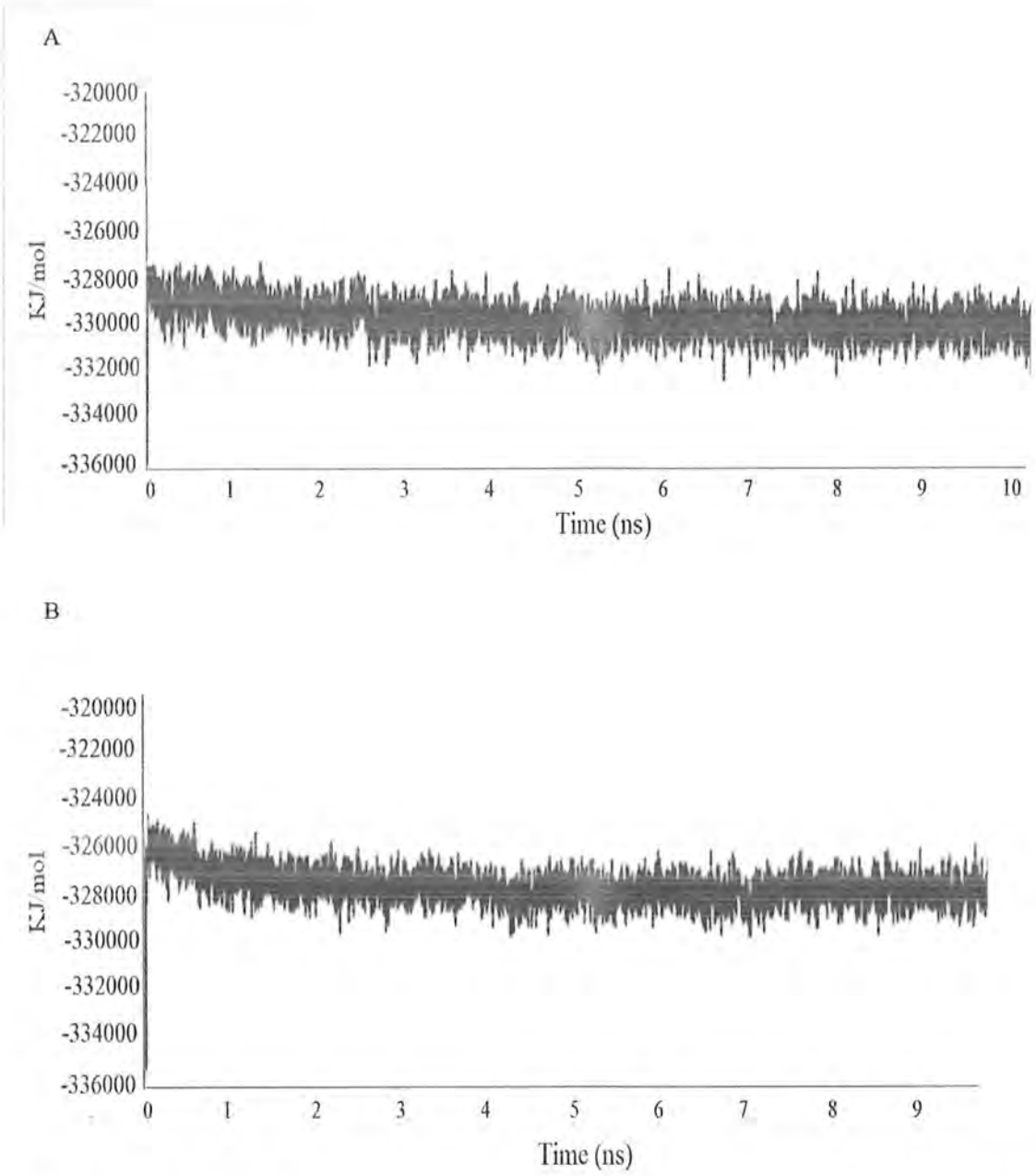

Figure 3.17: Energy plot. A shows $CX26^{WT}$-DPPC energy values, while B shows $CX26^{MUT}$-DPPC energy values at different time scale.

DISCUSSION

4. Discussion

Hearing loss is the third most common disorder in the world. In Pakistan, prevalence of hearing loss in 2014 was 7-8 per 1000 live births with an increasing rate every year (*http://tribune.com.pk/story/678415/disability-hearing-loss-deafness-on-the-rise/*).
Typically, sensorineural involves non-Syndromic deafness that doesn't include any other abnormality (Bitner-Glindzicz *et al.*, 2002). Non-syndromic deafness accounts for about 70% of genetic deafness and remaining cases are of syndromic deafness in which deafness is associated with other diseases such as Alport and Branchio-oto-renal etc. (Liu et al., 1997).

Multiple evidences indicate that mutations in *GJB2* gene; which encodes for Cx26 protein is one of the most leading causes of hearing loss (Ogawa *et al.*, 2007) accountable for >50% of non-syndromic deafness (Chen *et al.*, 2014). In this study our focus was to expolore the underlying cause of deafness due to T8M mutation in Cx26 as it is a major cause (6.1%) of deafness in Pakistan (Anjum *et al.*, 2014).

The interaction analysis of membrane proteins with membrane lipids is of structural and functional significance (Lee *et al.*, 2004). As a gap junctional protein, Cx26 is expressed in the inner ear such as the cochlea or the auditory nerve and provides a direct communication among adjacent cells to allow passage of 2nd messengers like ions (Ca^{2+} and K^{+} ions) or small molecules (IP3) across the membrane (Martin *et al.*, 1999). IP3 maintains the required ionic balance around the hair cells. IP3 activates the release of Ca^{2+} ions (Figure 4.1) which in turn maintains the balance of K^{+} ions around the hair cells. If Ca^{2+} ion concentration is low, it will imbalance the overall function (Figure 4.2). Any change in the structure of Cx26 may influence its interaction pattern with membrane lipids and lead to the disturbance in its regular passage of ions and small molecules, ultimately causing non-syndromic deafness.

By comparison of 2D and 3D structures of $Cx26^{WT}$ and $Cx26^{MUT}$, it was observed that T8M mutation completely disorganized the structure of $Cx26^{MUT}$, while $Cx26^{WT}$ structure was well organized and compact (Figures 3.1 and 3.2). In $Cx26^{MUT}$, multiple conformational

changes were observed i.e. absence of a β–sheet at Val52 and breakage of 1st transmembrane helix (TM1) at Trp44 that led to abrupt change in membrane topology of Cx26. Topology analysis illustrated two cytoplasmic and one extracellular loop in $Cx26^{WT}$ which exhibited both N- and C-termini in extracellular region, while $Cx26^{MUT}$ contained two extracellular and one cytoplasmic loops. Its N-terminus was localized in extracellular region, while C-terminus was present in the cytoplasmic region (Figure 3.3). The drastic change in structural topology led us to analyse pore and tunnel morphologies to determine their effects in the passage of 2nd messengers. Cx proteins are different due to their molecular weights and altered pore diameters. Normal pore diameter range for Cxs is 15-25Å (Harris *et al.*, 2001). Our analysis revealed the pore size of $Cx26^{WT}$ in the normal range (21.5Å), however, for $Cx26^{MUT}$, it reduced to 12Å (Figure 3.4). Similarly, Area profiles calculated for $Cx26^{WT}$ and $Cx26^{MUT}$ were 363Å^2 and 113Å^2, respectively (Figure 3.5).

Cx26 has a tunnel for the passage of 2nd messengers between adjacent cells. Tunnel starts from Asp2 leading to main pore at Lys41 and ends at Leu56 (Zonta *et al.*, 2012). Therefore, tunnel analysis for $Cx26^{WT}$ and $Cx26^{MUT}$ was performed which revealed the decrease of the tunnel length in $Cx26^{MUT}$. Results indicated disorganized and distorted tunnel in $Cx26^{MUT}$ at Lys41 which is an important pore residue, while in case of $Cx26^{WT}$, tunnel was well organized (Figure 3.6). In $Cx26^{MUT}$, length of tunnel was also decreased from 17.128Å to 14.4Å (Figure 3.7). These data indicated that T8M mutation drastically affected pore as well as tunnel characteristics of Cx26. This change in size and length of pore as well as tunnel may lead to narrowing of passage for 2nd messengers.

To further explore the stability as well as time-dependent behavior and dynamics of $Cx26^{WT}$ and $Cx26^{MUT}$ structures, MD simulations in lipid bilayer system (DPPC) were carried out. This approach helped to check the overall stability of $Cx26^{WT}$ and $Cx26^{MUT}$ proteins in lipid bilayer system of cell membrane. Individual $Cx26^{WT}$ without lipid bilayer system was taken as a reference.

$Cx26^{WT}$ exhibited strong binding with DPPC as compared to $Cx26^{MUT}$ (Figure 3.15). The RMSD, RMSF, hydrogen bonding and energy plots for both $Cx26^{WT}$ and $Cx26^{MUT}$ were generated. RMSD plot indicated that $Cx26^{WT}$ attained more stability than $Cx26^{MUT}$. Deviation of $Cx26^{WT}$ was upto 0.6Å (Figure 3.8), while it was upto 0.9Å for $Cx26^{MUT}$.

RMSF analysis revealed the fluctuating amino acid residues of $Cx26^{WT}$ and $Cx26^{MUT}$ in lipid bilayer system. The fluctuating residues were Gly12-Asn14, Thr18-Ile20, Leu56, Met93, Ala96 and Ile107-Gly109 which were located in loop region (Figure 3.12). RMSF analysis of DPPC was performed to evaluate fluctuations in lipid bilayer (DPPC). Major fluctuations included DPP79-DPP81, DPP4, DPP6, DPP101-DPP105, DPP110-DPP-112 and DPP126 (Figure 3.13). These residues were not involved in any interaction (Figure 3.15). Analysis of hydrogen bonds plot revealed that binding was increased after 0.5 ns for $Cx26^{WT}$-DPPC system and after 1.5 ns for $Cx26^{MUT}$-DPPC system. Overall, number of bonds were higher in $Cx26^{WT}$-DPPC as compared to $Cx26^{MUT}$-DPPC (Figure 3.16). These data indicated that $Cx26^{MUT}$ lost structural as well as functional features due to decreased binding of $Cx26^{MUT}$ and DPPC.

To check the overall stability of system, potential energy of a system, we plotted potential energy as a function of time. Resulted plot depicted that both systems were well equilibrated and remained stable throughout MD simulations. The $Cx26^{WT}$-DPPC (-328000 kcal/mol) system had shown lower potential energy values compared to $Cx26^{MUT}$-DPPC (-326000kcal/mol) complex (Figure 3.17).

It is important to analyse the entire environment for a large class of biomolecular processes, i.e., those that take place within biological membranes (Israelachvili *et al.*, 1980). We employed structural analysis as well as lipid bilayer simulation techniques to explore the behaviour of normal and T8M mutated Cx26 within lipid bilayer membrane. T8M mutation resulted structure instability and reduced functionality due to which 2^{nd} messenger are unable to pass through Cx26 creating functional disturbances leading to non-syndromic deafness.

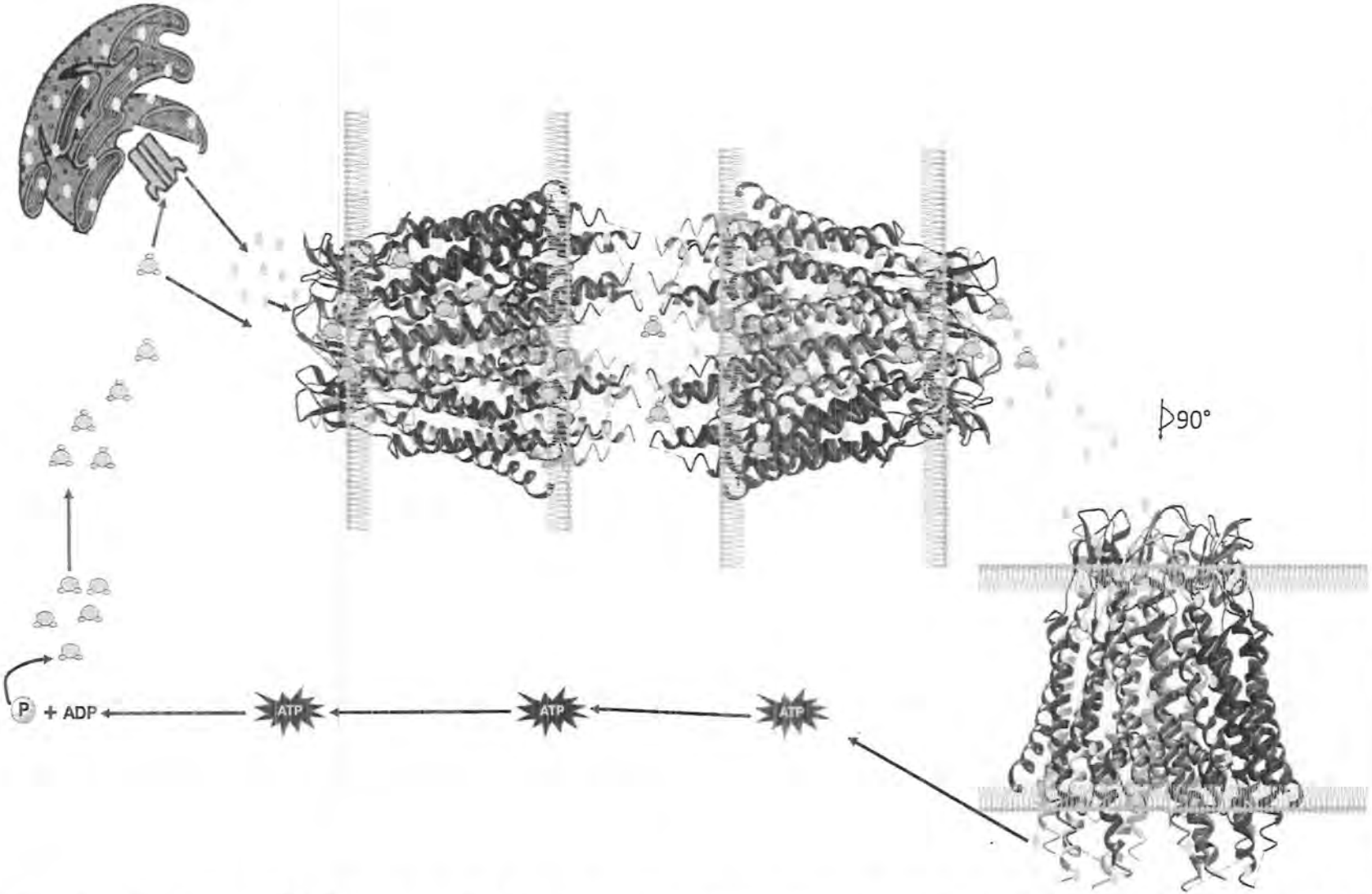

Figure 4.1: Pathway of Cx26^{WT} involved in hearing mechanism. IP3 diffuses across the cell, binds to an IP3 receptor and simulates Ca^{2+} ions release from endoplasmic reticulum. It generates an intracellular Ca^{2+} wave. Diffusion of IP3 through a gap junction to an adjacent cell initiates a 2nd intracellular Ca^{2+} wave. In addition, the stimulated cell releases ATP via hemichannels. This extracellular diffusion of ATP to adjacent cells activates P2 receptors which in turn, stimulate IP3 production to generate a $Ca2^{+}$ ion signal in the adjacent cell.

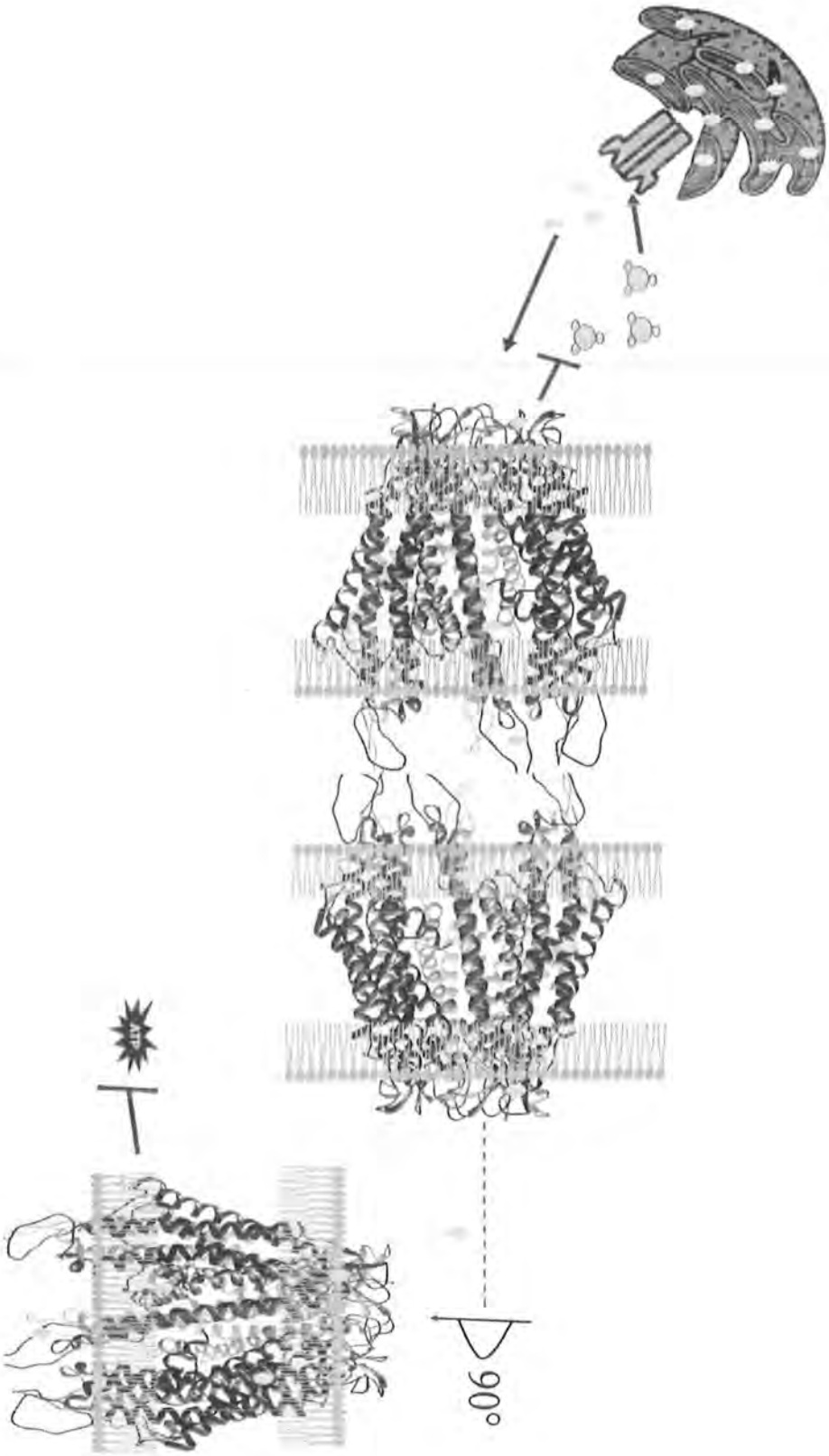

Figure 4.2: Pathway of Cx26^{MUT} in hearing mechanism. IP3 diffuses across the cell, binds to an IP3 receptor and simulate Ca^{2+} ions release from endoplasmic reticulum. It generates an intracellular Ca^{2+} wave. Diffusion of IP3 through a gap junction is inhibited due to T8M mutation and cell is unable to initiate a 2nd intracellular Ca^{2+} wave. It blocks the releases ATP for further process. This incomplete process ultimately causes non-syndromic deafness.

REFERENCES

5. Refrences

Ahmad, J. (2005). Identification of new gene involve in deafness in Pakistan population (Doctoral dissertation, University of the Punjab, Lahore).

Ahmed, Z. M., Li, X. C., Powell, S. D., Riazuddin, S., Young, T. L., Ramzan, K., & Wilcox, E. R. (2004). Characterization of a new full length TMPRSS3 isoform and identification of mutant alleles responsible for nonsyndromic recessive deafness in Newfoundland and Pakistan. BMC medical genetics, 5(1), 24.

Ahmed, Z. M., Masmoudi, S., Kalay, E., Belyantseva, I. A., Mosrati, M. A., Collin, R. W., & Kremer, H. (2008). Mutations of LRTOMT, a fusion gene with alternative reading frames, cause nonsyndromic deafness in humans. Nature genetics, 40(11), 1335-1340.

Ahmed, Z. M., Morell, R. J., Riazuddin, S., Gropman, A., Shaukat, S., Ahmad, M. M., & Wilcox, E. R. (2003). Mutations of MYO6 are associated with recessive deafness, DFNB37. The American Journal of Human Genetics, 72(5), 1315-1322.

Ahmed, Z. M., Yousaf, R., Lee, B. C., Khan, S. N., Lee, S., Lee, K., & Riazuddin, S. (2011). Functional null mutations of MSRB3 encoding methionine sulfoxide reductase are associated with human deafness DFNB74. The American Journal of Human Genetics, 88(1), 19-29.

Ali, G. (2010). Genetic deafness in Pakistani population. J Pak Med Assoc, 60, 418-419.

Anjum, S., Azhar, A., Tariq, M., Baig, S. M., Bolz, H. J., Qayyum, M., & Raja, G. K. (2014). GJB2 Gene Mutations Causing Hearing Loss in Consanguineous Pakistani Families. life, 12(3), 126-131.

Anwar, S., Riazuddin, S., Ahmed, Z. M., Tasneem, S., Khan, S. Y., Griffith, A. J., & Riazuddin, S. (2009). SLC26A4 mutation spectrum associated with DFNB4 deafness and Pendred's syndrome in Pakistanis. Journal of human genetics, 54(5), 266-270.

Arnold, K., Bordoli, L., Kopp, J., & Schwede, T. (2006). The SWISS-MODEL workspace: a web-based environment for protein structure homology modelling. Bioinformatics, 22(2), 195-201.

Baig, S. M., Koschak, A., Lieb, A., Gebhart, M., Dafinger, C., Nürnberg, G & Bolz, H. J. (2011). Loss of Cav1. 3 (CACNA1D) function in a human channelopathy with bradycardia and congenital deafness. Nature neuroscience, 14(1), 77-84.

Bandyopadhyay, S., Tarek, M., & Klein, M. L. (1999). Molecular dynamics study of a lipid-DNA complex. The Journal of Physical Chemistry B, 103(46), 10075-10080.

Baugh, E. H., Lyskov, S., Weitzner, B. D., & Gray, J. J. (2011). Real-time PyMOL visualization for Rosetta and PyRosetta. PloS one, 6(8), e21931.

Berendsen, H. J., van der Spoel, D., & van Drunen, R. (1995). GROMACS: A message-passing parallel molecular dynamics implementation. Computer Physics Communications, 91(1), 43-56.

Berman, H. M., Westbrook, J., Feng, Z., Gilliland, G., Bhat, T. N., Weissig, H., & Bourne, P. E. (2000). The protein data bank. Nucleic acids research, 28(1), 235-242.

Besold, G., Vattulainen, I., Karttunen, M., & Polson, J. M. (2000). Towards better integrators for dissipative particle dynamics simulations. Physical Review E, 62(6), R7611.

Birkenhager, R., Aschendorff, A., Schipper, J., & Laszig, R. (2007). [Non-syndromic hereditary hearing impairment]. Laryngo-rhino-otologie, 86(4), 299-309.

Bitner-Glindzicz, M. (2002). Hereditary deafness and phenotyping in humans. British medical bulletin, 63(1), 73-94.

Borck, G., Rehman, A. U., Lee, K., Pogoda, H. M., Kakar, N., von Ameln, S & Kubisch, C. (2011). Loss-of-function mutations of ILDR1 cause autosomal-recessive hearing impairment DFNB42. The American Journal of Human Genetics, 88(2), 127-137.

Bork, J. M., Peters, L. M., Riazuddin, S., Bernstein, S. L., Ahmed, Z. M., Ness, S. L., & Morell, R. J. (2001). Usher syndrome 1D and nonsyndromic autosomal recessive

deafness DFNB12 are caused by allelic mutations of the novel cadherin-like gene CDH23. The American Journal of Human Genetics, 68(1), 26-37.

Bosco, D., Haefliger, J. A., & Meda, P. (2011). Connexins: key mediators of endocrine function. Physiological reviews, 91(4), 1393-1445.

Brooks, C. L., Pettitt, B. M., & Karplus, M. (1990). Advances in Chemical Physics, Proteins: A Theoretical Perspective of Dynamics, Structure, and Thermodynamics. John Wiley & Sons.

Brown, K. A., Janjua, A. H., Karbani, G., Parry, G., Noble, A., Crockford, G., & Mueller, R. F. (1996). Linkage studies of non-syndromic recessive deafness (NSRD) in a family originating from the Mirpur region of Pakistan maps DFNB1 centromeric to D13S175. Human molecular genetics, 5(1), 169-173.

Bruzzone, R., White, T. W., & Paul, D. L. (1996). Connections with connexins: the molecular basis of direct intercellular signaling. In Ejb Reviews 1996 (pp. 135-161). Springer Berlin Heidelberg.

Carrasquillo, M. M., Zlotogora, J., Barges, S., & Chakravarti, A. (1997). Two different connexin 26 mutations in an inbred kindred segregating non-syndromic recessive deafness: implications for genetic studies in isolated populations. Human molecular genetics, 6(12), 2163-2172.

Chen, J., Chen, J., Zhu, Y., Liang, C., & Zhao, H. B. (2014). Deafness induced by Connexin 26 (GJB2) deficiency is not determined by endocochlear potential (EP) reduction but is associated with cochlear developmental disorders. Biochemical and biophysical research communications, 448(1), 28-32.

Chen, V. B., Arendall, W. B., Headd, J. J., Keedy, D. A., Immormino, R. M., Kapral, G. J., & Richardson, D. C. (2009). MolProbity: all-atom structure validation for macromolecular crystallography. Acta Crystallographica Section D: Biological Crystallography, 66(1), 12-21.

Chiu, S. W., Clark, M., Subramaniam, S., & Jakobsson, E. (2000). Collective motion artifacts arising in long-duration molecular dynamics simulations. Journal of Computational Chemistry, 21(2), 121-131.

Choi, B. Y., Ahmed, Z. M., Riazuddin, S., Bhinder, M. A., Shahzad, M., Husnain, T & Friedman, T. B. (2009). Identities and frequencies of mutations of the otoferlin gene (OTOF) causing DFNB9 deafness in Pakistan. Clinical genetics, 75(3), 237-243.

Chovancova, E., Pavelka, A., Benes, P., Strnad, O., Brezovsky, J., Kozlikova, B., & Biedermannova, L. (2012). CAVER 3.0: a tool for the analysis of transport pathways in dynamic protein structures.

Cohn, E. S., & Kelley, P. M. (1999). Clinical phenotype and mutations in connexin 26 (DFNB1/GJB2), the most common cause of childhood hearing loss. American journal of medical genetics, 89(3), 130-136.

Collin, R. W., Kalay, E., Tariq, M., Peters, T., van der Zwaag, B., Venselaar, H., & Kremer, H. (2008). Mutations of ESRRB encoding estrogen-related receptor beta cause autosomal-recessive nonsyndromic hearing impairment DFNB35. The American Journal of Human Genetics, 82(1), 125-138.

Cowtan, K. (2002). The clipper project. Joint CCP4 and ESF-EACBM Newsletter on Protein Crystallography, 40.

Cryns, K., & Van Camp, G. (2004). Deafness genes and their diagnostic applications. Audiology and Neurotology, 9(1), 2-22.

Davis, I. W., Murray, L. W., Richardson, J. S., & Richardson, D. C. (2004). MOLPROBITY: structure validation and all-atom contact analysis for nucleic acids and their complexes. Nucleic acids research, 32(suppl 2), W615-W619.

Dbouk, H. A., Mroue, R. M., El-Sabban, M. E., & Talhouk, R. S. (2009). Connexins: a myriad of functions extending beyond assembly of gap junction channels. Cell Commun Signal, 7(4), 10-1186.

Denoyelle, F., G. Lina-Granade, H. Plauchu, R. Bruzzone, H. Chaib, F. Levi-Acobas, D. Weil, C. Petit. (1998). Connexin 26 gene linked to a dominant deafness. Nature, 393, 319–320.

Denoyelle, F., Marlin, S., Weil, D., Moatti, L., Chauvin, P., Garabedian, E. N., & Petit, C. (1999). Clinical features of the prevalent form of childhood deafness, DFNB1, due to a connexin-26 gene defect: implications for genetic counselling. The Lancet, 353(9161), 1298-1303.ke

Denoyelle, F., Weil, D., Maw, M. A., Wilcox, S. A., Lench, N. J., Allen-Powell, D. R., & Petit, C. (1997). Prelingual deafness: high prevalence of a 30delG mutation in the connexin 26 gene. Human molecular genetics, 6(12), 2173-2177.

Emsley, P., & Cowtan, K. (2004). Coot: model-building tools for molecular graphics. Acta Crystallographica Section D: Biological Crystallography, 60(12), 2126-2132.

Emsley, P., Lohkamp, B., Scott, W. G., & Cowtan, K. (2010). Features and development of Coot. Acta Crystallographica Section D: Biological Crystallography, 66(4), 486-501.

Estivill, X., Fortina, P., Surrey, S., Rabionet, R., Melchionda, S., D'Agruma, L., & Gasparini, P. (1998). Connexin-26 mutations in sporadic and inherited sensorineural deafness. The Lancet, 351(9100), 394-398.

Eswar, N., Eramian, D., Webb, B., Shen, M. Y., & Sali, A. (2008). Protein structure modeling with MODELLER. In Structural Proteomics (pp. 145-159). Humana Press.

Eswar, N., Webb, B., Marti-Renom, M. A., Madhusudhan, M. S., Eramian, D., Shen, M. Y., & Sali, A. (2006). Comparative protein structure modeling using Modeller. Current protocols in bioinformatics, 5-6.

Feller, S. E., Gawrisch, K., & MacKerell, A. D. (2002). Polyunsaturated fatty acids in lipid bilayers: intrinsic and environmental contributions to their unique physical properties. Journal of the American Chemical Society, 124(2), 318-326.

Flicek, P., Amode, M. R., Barrell, D., Beal, K., Brent, S., Carvalho-Silva, D., & Gil, L. (2011). Ensembl 2012. Nucleic acids research, gkr991.

Friedman, T. B., & Griffith, A. J. (2003). Human Nonsyndromic Sensorineural Deafness. Annual review of genomics and human genetics, 4(1), 341-402.

Fujita, P. A., Rhead, B., Zweig, A. S., Hinrichs, A. S., Karolchik, D., Cline, M. S., & Diekhans, M. (2010). The UCSC genome browser database: update 2011. Nucleic acids research, gkq963.

Goddard, T. D., Huang, C. C., & Ferrin, T. E. (2007). Visualizing density maps with UCSF Chimera. Journal of structural biology, 157(1), 281-287.

Green, G. E., Scott, D. A., McDonald, J. M., Woodworth, G. G., Sheffield, V. C., & Smith, R. J. (1999). Carrier rates in the midwestern United States for GJB2 mutations causing inherited deafness. Jama, 281(23), 2211-2216.

Gumbart, J., Wang, Y., Aksimentiev, A., Tajkhorshid, E., & Schulten, K. (2005). Molecular dynamics simulations of proteins in lipid bilayers. Current opinion in structural biology, 15(4), 423-431.

Haile, J. M. (1992). Molecular dynamics simulation (Vol. 18). Wiley, New York.

Harris, A. (2001). Emerging issues of connexin channels: biophysics fills the gap. Quarterly reviews of biophysics, 34(03), 325-472.

Harris, A., & Locke, D. (Eds.). (2008). Connexins: a guide. Springer Science & Business Media.

Hess, B., Kutzner, C., Van Der Spoel, D., & Lindahl, E. (2008). GROMACS 4: algorithms for highly efficient, load-balanced, and scalable molecular simulation. Journal of chemical theory and computation, 4(3), 435-447.

Hilgert, N., Smith, R. J., & Van Camp, G. (2009). Forty-six genes causing nonsyndromic hearing impairment: which ones should be analyzed in DNA diagnostics?. Mutation Research/Reviews in Mutation Research, 681(2), 189-196.

Hubbard, T., Barker, D., Birney, E., Cameron, G., Chen, Y., Clark, L., & Durbin, R. (2002). The Ensembl genome database project. Nucleic acids research, 30(1), 38-41.

Hussain, R., & Bittles, A. H. (1998). The prevalence and demographic characteristics of consanguineous marriages in Pakistan. Journal of biosocial science, 30(02), 261-275.

Ibragimova, G. T., & Wade, R. C. (1998). Importance of explicit salt ions for protein stability in molecular dynamics simulation. Biophysical journal, 74(6), 2906-2911.

Israelachvili, J. N., Marcelja, S., & Horn, R. G. (1980). Physical principles of membrane organization. Quarterly reviews of biophysics, 13(02), 121-200.

Karolchik, D., Barber, G. P., Casper, J., Clawson, H., Cline, M. S., Diekhans, M., & Harte, R. A. (2014). The UCSC genome browser database: 2014 update. Nucleic acids research, 42(D1), D764-D770.

Kelley, P. M., Cohn, E., & Kimberling, W. J. (2000). Connexin 26: required for normal auditory function. Brain research reviews, 32(1), 184-188.

Kelley, P. M., Harris, D. J., Comer, B. C., Askew, J. W., Fowler, T., Smith, S. D., & Kimberling, W. J. (1998). Novel mutations in the connexin 26 gene (GJB2) that cause autosomal recessive (DFNB1) hearing loss. The American Journal of Human Genetics, 62(4), 792-799.

Kelsell, D. P., Dunlop, J., Stevens, H. P., Lench, N. J., Liang, J. N., Parry, G., & Leigh, I. M. (1997). Connexin 26 mutations in hereditary non-syndromic sensorineural deafness. Nature, 387(6628), 80-83.

Kemperman, M. H., Hoefsloot, L. H., & Cremers, C. W. (2002). Hearing loss and connexin 26. Journal of the Royal Society of Medicine, 95(4), 171-177.

Khan, S. Y., Ahmed, Z. M., Shabbir, M. I., Kitajiri, S. I., Kalsoom, S., Tasneem, S., & Riazuddin, S. (2007). Mutations of the RDX gene cause nonsyndromic hearing loss at the DFNB24 locus. Human mutation, 28(5), 417-423.

Kikuchi, T., Kimura, R. S., Paul, D. L., Takasaka, T., & Adams, J. C. (2000). Gap junction systems in the mammalian cochlea. Brain research reviews, 32(1), 163-166.

Kitajiri, S., McNamara, R., Makishima, T., Husnain, T., Zafar, A. U., Kittles, R. A., & Griffith, A. J. (2007). Identities, frequencies and origins of TMC1 mutations causing DFNB7/B11 deafness in Pakistan. Clinical genetics, 72(6), 546-550.

Kozlikova, B., Sebestova, E., Sustr, V., Brezovsky, J., Strnad, O., Daniel, L., & Benes, P. (2014). CAVER Analyst 1.0: graphic tool for interactive visualization and analysis of tunnels and channels in protein structures.Bioinformatics, 30(18), 2684-2685.

Krieger, E., & Vriend, G. (2014). YASARA View—molecular graphics for all devices—from smartphones to workstations. Bioinformatics, 30(20), 2981-2982.

Krieger, E., Joo, K., Lee, J., Lee, J., Raman, S., Thompson, J & Karplus, K. (2009). Improving physical realism, stereochemistry, and side-chain accuracy in homology modeling: four approaches that performed well in CASP8. Proteins: Structure, Function, and Bioinformatics, 77(S9), 114-122.

Laird, D. (2006). Life cycle of connexins in health and disease. Biochem. J, 394, 527-543.

Laskowski, R. A., & Swindells, M. B. (2011). LigPlot+: multiple ligand–protein interaction diagrams for drug discovery. Journal of chemical information and modeling, 51(10), 2778-2786.

Lawrence, T. S., Beers, W. H., & Gilula, N. B. (1978). Transmission of hormonal stimulation by cell-to-cell communication.

Lee, A. G. (2004). How lipids affect the activities of integral membrane proteins. Biochimica et Biophysica Acta (BBA)-Biomembranes, 1666(1), 62-87.

Liu, X. Z., Walsh, J., Mburu, P., Kendrick-Jones, J., Cope, M. J. T., Steel, K. P., & Brown, S. D. (1997). Mutations in the myosin VIIA gene cause non-syndromic recessive deafness. Nature genetics, 16(2), 188-190.

Locke, D., & Harris, A. L. (2009). Connexin channels and phospholipids: association and modulation. BMC biology, 7(1), 52.

Maeda, S., Nakagawa, S., Suga, M., Yamashita, E., Oshima, A., Fujiyoshi, Y., & Tsukihara, T. (2009). Structure of the connexin 26 gap junction channel at 3.5 Å resolution. Nature, 458(7238), 597-602.

Malewicz, Barbara, V. V. Kumar, Ross G. Johnson, and Wolfgang J. Baumann. "Lipids in gap junction assembly and function." Lipids 25, no. 8 (1990): 419-427.

Martin, P. E., Coleman, S. L., Casalotti, S. O., Forge, A., & Evans, W. H. (1999). Properties of connexin26 gap junctional proteins derived from mutations associated with non-syndromal heriditary deafness. Human molecular genetics,8(13), 2369-2376.

Meng, E. C., Pettersen, E. F., Couch, G. S., Huang, C. C., & Ferrin, T. E. (2006). Tools for integrated sequence-structure analysis with UCSF Chimera.BMC bioinformatics, 7(1), 339.

Mooney, C. Z. (1997). Monte carlo simulation (Vol. 116). Sage Publications.

Morton, N. E. (1991). Genetic epidemiology of hearing impairment. Annals of the New York Academy of Sciences, 630(1), 16-31.

Mujtaba, G., Bukhari, I., Fatima, A., & Naz, S. (2012). A p. C343S missense mutation in PJVK causes progressive hearing loss. Gene, 504(1), 98-101.

Murgia, A., Orzan, E., Polli, R., Martella, M., Vinanzi, C., Leonardi, E., & Zacchello, F. (1999). Cx26 deafness: mutation analysis and clinical variability. Journal of medical genetics, 36(11), 829-832.

Nal, N., Ahmed, Z. M., Erkal, E., Alper, O. M., Lüleci, G., Dinç, O., & Riazuddin, S. (2007). Mutational spectrum of MYO15A: the large N-terminal extension of myosin XVA is required for hearing. Human mutation, 28(10), 1014.

Nayak, G., Varga, L., Trincot, C., Shahzad, M., Friedman, P. L., Klimes, I & Riazuddin, S. (2015). Molecular genetics of MARVELD2 and clinical phenotype in Pakistani and Slovak families segregating DFNB49 hearing loss. Human genetics, 134(4), 423-437.

Naz, S., Giguere, C. M., Kohrman, D. C., Mitchem, K. L., Riazuddin, S., Morell, R. J., & Wilcox, E. R. (2002). Mutations in a novel gene, TMIE, are associated with hearing loss linked to the DFNB6 locus. The American Journal of Human Genetics, 71(3), 632-636.

Ogawa, H., Suzutan, T., Baba, Y., Koyano, S., Nozawa, N., Ishibashi, K., & Omori, K. (2007). Etiology of severe sensorineural hearing loss in children: independent impact of congenital cytomegalovirus infection and GJB2 mutations. Journal of Infectious Diseases, 195(6), 782-788.

Padma, G., Ramchander, P. V., Nandur, U. V., & Padma, T. (2009). GJB2 and GJB6 gene mutations found in Indian probands with congenital hearing impairment. Journal of genetics, 88(3), 267-272.

Pandit, S. A., & Berkowitz, M. L. (2002). Molecular dynamics simulation of dipalmitoylphosphatidylserine bilayer with Na+ counterions. Biophysical journal, 82(4), 1818-1827.

Park, H. J., Shaukat, S., Liu, X. Z., Hahn, S. H., Naz, S., Ghosh, M., & Griffith, A. J. (2003). Origins and frequencies of SLC26A4 (PDS) mutations in east and south Asians: global implications for the epidemiology of deafness. Journal of medical genetics, 40(4), 242-248.

Pastor, R. W. (1994). Molecular dynamics and Monte Carlo simulations of lipid bilayers. Current Opinion in Structural Biology, 4(4), 486-492.

Petrek, M., Otyepka, M., Banáš, P., Košinová, P., Koča, J., & Damborský, J. (2006). CAVER: a new tool to explore routes from protein clefts, pockets and cavities. BMC bioinformatics, 7(1), 316.

Pettersen, E. F., Goddard, T. D., Huang, C. C., Couch, G. S., Greenblatt, D. M., Meng, E. C., & Ferrin, T. E. (2004). UCSF Chimera—a visualization system for exploratory research and analysis. Journal of computational chemistry, 25(13), 1605-1612

Pronk, S., Páll, S., Schulz, R., Larsson, P., Bjelkmar, P., Apostolov, R., & Hess, B. (2013). GROMACS 4.5: a high-throughput and highly parallel open source molecular simulation toolkit. Bioinformatics, btt055.

Rabionet, R., S. Melchionda, L. D'Agruma, L. Zelante, P. Gasparini,. S. Estivill. (1998). Mutations in the connexin 26 gene GJB2 in Italian and Spanish patients with congenital deafness. Am. J. Hum. Genet, 63, A381, Abstr.

Rehman, A. U., Morell, R. J., Belyantseva, I. A., Khan, S. Y., Boger, E. T., Shahzad, M., & Friedman, T. B. (2010). Targeted capture and next-generation sequencing identifies C9orf75, encoding taperin, as the mutated gene in nonsyndromic deafness DFNB79. The American Journal of Human Genetics, 86(3), 378-388.

Retamal, M. A., Reyes, E. P., García, I. E., Pinto, B., Martínez, A. D., & González, C. (2015). Diseases associated with leaky hemichannels. Frontiers in cellular neuroscience, 9.

Riaz, A., & Iqbal, M. (2012). Non-syndromic autosomal recessive deafness in Pakistani population: Epidemiology and genetics. Pakistan J. Zool, 44(6), 1431-1438.

Riazuddin, S., Belyantseva, I. A., Giese, A. P., Lee, K., Indzhykulian, A. A., Nandamuri, S. P., & Ahmed, Z. M. (2012). Alterations of the CIB2 calcium-and integrin-binding protein cause Usher syndrome type 1J and nonsyndromic deafness DFNB48. Nature genetics, 44(11), 1265-1271.

Riazuddin, S., Khan, S. N., Ahmed, Z. M., Ghosh, M., Caution, K., Nazli, S., & Friedman, T. B. (2006). Mutations in TRIOBP, which encodes a putative cytoskeletal-organizing protein, are associated with nonsyndromic recessive deafness. The American Journal of Human Genetics, 78(1), 137-143.

Riazuddin, S., Nazli, S., Ahmed, Z. M., Yang, Y., Zulfiqar, F., Shaikh, R. S & Friedman, T. B. (2008). Mutation spectrum of MYO7A and evaluation of a novel nonsyndromic deafness DFNB2 allele with residual function. Human mutation, 29(4), 502.

Saez, J. C., Berthoud, V. M., Branes, M. C., Martinez, A. D., & Beyer, E. C. (2003). Plasma membrane channels formed by connexins: their regulation and functions. Physiological reviews, 83(4), 1359-1400.

Saiz, L., & Klein, M. L. (2001). Structural properties of a highly polyunsaturated lipid bilayer from molecular dynamics simulations. Biophysical journal, 81(1), 204-216.

Sali, A., Potterton, L., Yuan, F., van Vlijmen, H., & Karplus, M. (1995). Evaluation of comparative protein modeling by MODELLER. Proteins: Structure, Function, and Bioinformatics, 23(3), 318-326.

Santos, R. L. P., Wajid, M., Khan, M. N., McArthur, N., Pham, T. L., Bhatti, A., & Leal, S. M. (2005). Novel sequence variants in the TMC1 gene in Pakistani families with autosomal recessive hearing impairment. Human mutation, 26(4), 396-396.

Schultz, J. M., Khan, S. N., Ahmed, Z. M., Riazuddin, S., Waryah, A. M., Chhatre, D & Morell, R. J. (2009). Noncoding mutations of HGF are associated with nonsyndromic hearing loss, DFNB39. The American Journal of Human Genetics, 85(1), 25-39.

Scott, D. A., Kraft, M. L., Carmi, R., Ramesh, A., Elbedour, K., Yairi, Y., & Sheffield, V. C. (1998). Identification of mutations in the connexin 26 gene that cause autosomal recessive nonsyndromic hearing loss. Human mutation, 11(5), 387.

Scott, D. A., Kraft, M. L., Stone, E. M., Sheffield, V. C., & Smith, R. J. (1998). Connexin mutations and hearing loss. Nature, 391(6662), 32-32.

Snoeckx, R. L., Huygen, P. L., Feldmann, D., Marlin, S., Denoyelle, F., Waligora, J., & Gronskov, K. (2005). GJB2 mutations and degree of hearing loss: a multicenter study. The American Journal of Human Genetics, 77(6), 945-957.

Sohl, G., Eiberger, J., Jung, Y. T., Kozak, C. A., & Willecke, K. (2001). The mouse gap junction gene connexin29 is highly expressed in sciatic nerve and regulated during brain development. Biological chemistry, 382(6), 973-978.

Spyropoulos, I. C., Liakopoulos, T. D., Bagos, P. G., & Hamodrakas, S. J. (2004). TMRPres2D: high quality visual representation of transmembrane protein models. Bioinformatics, 20(17), 3258-3260.

Terwilliger, T. C. (1982). The helical hydrophobic moment: a measure of the amphiphilicity of a helix. Nature, 299, 371-374.

Tieleman, D. P., Marrink, S. J., & Berendsen, H. J. (1997). A computer perspective of membranes: molecular dynamics studies of lipid bilayer systems. Biochimica et Biophysica Acta (BBA)-Reviews on Biomembranes, 1331(3), 235-270.

Tobias, D. J. (2001). Electrostatics calculations: recent methodological advances and applications to membranes. Current opinion in structural biology, 11(2), 253-261.

Traynor, B. (2011). The incidence of hearing loss around the world. Hearing International.

Van Camp, G., & Smith, R. J. H. Hereditary Hearing Loss Homepage 2012. URL: http://hereditaryhearingloss. org.

Van Der Spoel, D., Lindahl, E., Hess, B., Groenhof, G., Mark, A. E., & Berendsen, H. J. (2005). GROMACS: fast, flexible, and free. Journal of computational chemistry, 26(16), 1701-1718.

Van-Naarden, K., Decouflé, P., & Caldwell, K. (1999). Prevalence and characteristics of children with serious hearing impairment in metropolitan Atlanta, 1991–1993. Pediatrics, 103(3), 570-575.

Vattulainen, I., Karttunen, M., Besold, G., & Polson, J. M. (2002). Integration schemes for dissipative particle dynamics simulations: From softly interacting systems towards hybrid models. The Journal of chemical physics, 116(10), 3967-3979.

Venable, R. M., Brooks, B. R., & Pastor, R. W. (2000). Molecular dynamics simulations of gel (LβI) phase lipid bilayers in constant pressure and constant surface area ensembles. The Journal of Chemical Physics, 112(10), 4822-4832.

Vinken, M., Vanhaecke, T., Papeleu, P., Snykers, S., Henkens, T., & Rogiers, V. (2006). Connexins and their channels in cell growth and cell death. Cellular signalling, 18(5), 592-600.

Wallace, A. C., Laskowski, R. A., & Thornton, J. M. (1995). LIGPLOT: a program to generate schematic diagrams of protein-ligand interactions.Protein engineering, 8(2), 127-134.

Waryah, A. M., Rehman, A., Ahmed, Z. M., Bashir, Z. H., Khan, S. Y., Zafar, A. U., & Friedman, T. B. (2009). DFNB74, a novel autosomal recessive nonsyndromic hearing impairment locus on chromosome 12q14. 2-q15. Clinical genetics, 76(3), 270-275.

Wesson, L., & Eisenberg, D. (1992). Atomic solvation parameters applied to molecular dynamics of proteins in solution. Protein science: a publication of the Protein Society, 1(2), 227.

White, T. W., Deans, M. R., Kelsell, D. P., & Paul, D. L. (1998). Connexin mutations in deafness. Nature, 394(6694), 630-631.

Xu, J., & Nicholson, B. J. (2013). The role of connexins in ear and skin physiology—functional insights from disease-associated mutations. Biochimica et Biophysica Acta (BBA)-Biomembranes, 1828(1), 167-178.

Yang, Z., Lasker, K., Schneidman-Duhovny, D., Webb, B., Huang, C. C., Pettersen, E. F., & Ferrin, T. E. (2012). UCSF Chimera, MODELLER, and IMP: an integrated modeling system. Journal of structural biology, 179(3), 269-278.

Yilmaz, A., Menevse, S., Bayazit, Y., Karamert, R., Ergin, V., & Menevse, A. (2010). Two novel missense mutations in the connexin 26 gene in Turkish patients with nonsyndromic hearing loss. Biochemical genetics, 48(3-4), 248-256.

Zakzouk, S. (2002). Consanguinity and hearing impairment in developing countries: a custom to be discouraged. The Journal of Laryngology & Otology, 116(10), 811-816.

Zelante, L., Gasparini, P., Estivill, X., Melchionda, S., D'Agruma, L., Govea, N., & Fortina, P. (1997). Connexin26 mutations associated with the most common form of non-syndromic neurosensory autosomal recessive deafness (DFNB1) in Mediterraneans. Human molecular genetics, 6(9), 1605-1609.

Zheng, Q. Y., Yan, D., Ouyang, X. M., Du, L. L., Yu, H., Chang, B & Liu, X. Z. (2005). Digenic inheritance of deafness caused by mutations in genes encoding cadherin 23 and protocadherin 15 in mice and humans. Human molecular genetics, 14(1), 103-111.

Zonta, F., Polles, G., Zanotti, G., & Mammano, F. (2012). Permeation pathway of homomeric connexin 26 and connexin 30 channels investigated by molecular dynamics. Journal of Biomolecular Structure and Dynamics, 29(5), 985-998.